

NPS ARCHIVE
1963
HAGGQUIST, G.

PLASMA RESONANCE IN
ARGON AND NEON
GRANT F. HAGGQUIST

LIBRARY
U.S. NAVAL POSTGRADUATE SCHOOL
MONTEREY CALIFORNIA

DUDLEY KNOX LIBRARY
NAVAL POSTGRADUATE SCHOOL
MONTEREY CA 93943-5101

PLASMA RESONANCE
IN
ARGON AND NEON

* * * *

Grant F. Haggquist, Jr.

PLASMA RESONANCE

IN

ARGON AND NEON

by

Grant F. Haggquist, Jr.

Lieutenant Commander, United States Navy

Submitted in partial fulfillment of
the requirements for the degree of

MASTER OF SCIENCE
IN
PHYSICS

United States Naval Postgraduate School
Monterey, California

1 9 6 3

PLASMA RESONANCE

IN

ARGON AND NEON

by

Grant F. Haggquist, Jr.

This work is accepted as fulfilling
the thesis requirements for the degree of

MASTER OF SCIENCE

IN

PHYSICS

from the

United States Naval Postgraduate School

ABSTRACT

Plasma resonance in argon and neon was studied by a microwave method which afforded a measure of the electron number density. Resonance was excited by an R. F. signal transmitted along a strip-line enclosing the discharge tube. The resonance occurrence was determined by measuring the transmitted power as a function of discharge current and exciting frequency. Data are presented showing the current for resonance as a function of resonant frequency for several gas pressures. In argon, measurements were made for pressure in the range from 1×10^{-3} to 5×10^{-2} mm Hg. In neon the pressure range was 1×10^{-2} to 7×10^{-1} mm Hg. The upper pressure limit was determined by the Q of the resonance and the lower limit only by ability to maintain a normal glow discharge. The large pressure range for neon suggests that this method of determining the electron number density should find many applications in work using that gas.

ACKNOWLEDGMENTS

The writer wishes to express his gratitude to Professor Norman L. Oleson for his encouragement, guidance, and many helpful suggestions during the course of this work. Especial appreciation is extended to Professor Gordon S. Kino and Mr. Sidney A. Self of the Microwave Laboratory, W. W. Hanson Laboratories of Physics, Stanford University, where the writer spent a part of the summer 1962 and obtained knowledge of the techniques necessary to this work. Professor A. W. M. Cooper's ever ready assistance in vacuum system construction and modification is also most appreciated. Thanks are given to Messrs. John M. Calder, Harold Harriman, Robert Smith and Peter Wisler for assistance in construction of the experimental equipment.

TABLE OF CONTENTS

Section	Title	Page
1.	Introduction	1
2.	The Analysis of Crawford, Kino, Self and Spaulter	5
3.	Experimental Method	7
4.	Equipment	9
5.	Procedures	19
6.	Results and Discussion	22
7.	Recommendations	28
	Bibliography	53
	Appendix	54

LIST OF ILLUSTRATIONS

Figure		Page
1.	Dielectric cylinder in an uniform electric field	29
2.	Ideal resonating system	30
3.	Experimental equipment arrangement	31
4.	Experimental discharge tube	32
5.	Experimental circuitry	33
6.	Current modulation circuit	34
7.	Strip-line assembly	35
8.	Typical resonance	36
9.	Subsidiary resonance	37
10.	Resonance in Tube I	38
11.	Resonance in Tube II	39
12.	Effect of pressure on resonance in Tube I with neon	40
13.	Effect of discharge current on resonance in Tube I with neon at pressure of 2.1×10^{-1} mm Hg.	41
14.	Current for resonance vs inverse pressure. Argon in Tube I	42
15.	Current for resonance vs inverse pressure. Neon in Tube I	43
16.	Current for resonance vs inverse pressure. Argon in Tube II	44
17.	Current for resonance vs resonant frequency. Argon in Tube I	45
18.	Current for resonance vs resonant frequency. Neon in Tube I	46

LIST OF ILLUSTRATIONS

Figure		Page
19.	Current for resonance vs resonant frequency. Argon in Tube II	47
20.	Tube characteristic for neon at approximately 1×10^{-2} mm Hg	48
21.	Anomalous resonance	49
22.	Variation of pressure with discharge current in argon	50
23.	Calibration curve for argon. Westinghouse 7903 ion gauge	51
24.	Calibration curve for neon. Westinghouse 7903 ion gauge	52

1. Introduction

The systematic study of the plasma resonance was initiated by Tonks¹ in 1929-31. Tonks² defined two types of plasma resonance, one called "plasma-electron resonance" and the other just "plasma resonance". The "plasma-electron resonance" was defined as a completely internal oscillation with frequency dependent only on the electron density. The frequency of this resonance (or oscillation) is given by the well known plasma frequency. "Plasma resonance", as defined by Tonks, is the resonance of the plasma in response to a definite field configuration. This is the type of resonance considered in this work.

The phenomenon of plasma resonance can be described with a simple model. Consider an infinitely long, circularly cylindrical, uniform plasma column. Perpendicularly to the axis of the column is impressed a uniform electric field of frequency ω given by

$$E_x = E_{0x} e^{j\omega t} . \quad (1)$$

Neglecting collisions, the equation of motion for the electrons in the plasma column is

$$\frac{d^2x}{dt^2} = \frac{-eE_x}{m_e} = \frac{-eE_{0x} e^{j\omega t}}{m_e} . \quad (2)$$

The electron velocity is then

$$v = \frac{dx}{dt} = \frac{-eE_{0x} e^{j\omega t}}{j\omega m_e} = \frac{-eE_x}{j\omega m_e} , \quad (3)$$

and the electron current density

$$\mathbf{J} = -n_e e v = \frac{n_e e^2 E_x}{j \omega m_e} . \quad (4)$$

Now Maxwell's curl equation for the magnetic field intensity is, in free space

$$\nabla \times \vec{H} = \vec{J} + \epsilon_0 \frac{d\vec{E}}{dt} \quad (5)$$

Then from equations (1) and (4), equation (5) becomes

$$\begin{aligned} (\nabla \times \vec{H})_x &= \frac{n_e e^2 E_x}{j \omega m_e} + j \omega \epsilon_0 E_x \\ &= j \omega \left(\epsilon_0 - \frac{n_e e^2}{m_e \omega^2} \right) E_x . \end{aligned} \quad (6)$$

This is the equation for a polarizable medium of permittivity

$$\epsilon = \epsilon_0 - \frac{n_e e^2}{m_e \omega^2} , \quad (7)$$

and dielectric constant

$$K = 1 - \frac{n_e e^2}{\epsilon_0 m_e \omega^2} . \quad (8)$$

Introducing the well known plasma frequency

$$\omega_p^2 = \frac{n_e e^2}{m_e \epsilon_0} \quad (9)$$

the dielectric constant becomes

$$K = 1 - \frac{\omega_p^2}{\omega^2} \quad (10)$$

Thus a plasma of permittivity ϵ_0 and electron current J may be considered as a dielectric with no electron current and permittivity given by equation (7).

Now consider an infinite dielectric, circularly cylindrical, column of dielectric constant K in an uniform electric field E_0 . It can be shown³ that the field inside the column, E_i , is related to the field outside, E_0 , by

$$E_i = \frac{2 E_0}{1 + K} \quad (11)$$

The field distribution is as shown in Fig. 1. From equation (11) it is seen that the field inside the column becomes infinitely large as K approaches the value -1 . In reality, collisions in the plasma introduce losses and the field E_i remains finite. This is the condition of resonance and from equation (10) it occurs when the impressed frequency is related to the plasma frequency ω_p by

$$\omega = \omega_p / \sqrt{2} \quad . \quad (12)$$

Thus, a strong power absorption from the external field into the plasma is expected when equation (12) is satisfied.

This type of resonance has been studied by many workers. Typical among them is Rommel⁴, who measured the reflection of radio waves from a plasma column suspended in free space, and Dattner⁵, who measured the transmitted power through a waveguide in which a plasma column was mounted. Crawford, Kino, Self, and Spaulter⁶ developed a method of observing this resonance by replacing the waveguide with an

easily-constructed strip-line . All the above workers used a low-pressure mercury vapor discharge to provide the plasma . In this work , the method of Crawford , et al,⁶ is used with plasmas of argon and neon .

2. The Analysis of Crawford, Kino, Self, and Spaulter

The previous model of an uniform plasma and an uniform field is impossible to achieve in the laboratory so a more practical system must be devised. Based on the ideal resonating system of Fig. 2, Crawford, Kino, Self, and Spalter⁶ have derived by means of a variation principle an expression of the form

$$\omega_0^2 = \omega_{p0}^2 \frac{k_2}{k_1} \quad (13)$$

where ω_0 is the resonant frequency and ω_{p0} is the plasma frequency on the axis of the column.

The constant, k_2 , depends on the number of azimuthal field variations ($2m$) and the radial variation of electron number density assumed. A parabolic variation of the form

$$\omega_p^2 = \omega_{p0}^2 \left[1 - \left(\frac{r}{a} \right)^2 \right] \quad (14)$$

where ω_p is the plasma frequency at a distance r from the axis, was employed in the analysis. The constant, k_2 , is given by

$$k_2 = 1 - \alpha \left(\frac{m}{m+1} \right) \quad (15)$$

The constant, k_1 , depends on the geometry of the system and takes into account the effects of the electrodes providing the field, the glass tube containing the plasma column and the azimuthal field variations. For the geometry shown in Fig. 2, k_1 is given by

$$k_2 = 1 + K_1 \left[\frac{1 - \left(\frac{1-\delta}{1+\delta} \right) \left(\frac{a}{b} \right)^{2m}}{1 + \left(\frac{1-\delta}{1+\delta} \right) \left(\frac{a}{b} \right)^{2m}} \right] \quad (16)$$

where

$$\delta = \frac{K_2}{K_1} \left(\frac{1 + \left(\frac{b}{c} \right)^{2m}}{1 - \left(\frac{b}{c} \right)^{2m}} \right)$$

Practical formulae derived from equations (13) and (9) give either the number density, n_0 , on the axis, or \bar{n} the mean value across the column:

$$n_0 = 1.24 \left(\frac{k_1}{k_2} \right) f_0^2 \quad 10^{-8} / \text{cm}^3 \quad (17a)$$

(For any m)

$$\bar{n} = 1.24 k_1 f_0^2 \quad 10^{-8} / \text{cm}^3 \quad (17b)$$

(For m = 1 only)

where the resonant frequency, f_0 , is in c/s.

The theoretical Q of the resonating system was shown to be

$$Q = \frac{\omega_0}{\nu} \quad (18)$$

where ν is the elastic collision frequency for electrons and neutrals.

3. Experimental Method

The electron current in the discharge tube is given by

$$I = \bar{n}_e A e \bar{v} \quad (19)$$

where \bar{n}_e is the mean electron density, A is the discharge tube cross-section, and \bar{v} is the mean electron drift velocity. The mean velocity \bar{v} is a function of $(E/p)^{7/2}$ and in a low pressure, normal glow discharge, the current is constant or at most a slowly varying function of E . It then will be assumed that

$$I \sim \bar{n}_e . \quad (20)$$

The validity of this assumption is verified in the section on Results. Equations (9), (13), (17), and (20) provide the means for experimentally determining the electron number density as a function of discharge tube current. Combining equations (9), (13), and (17) we have

$$I \sim \omega_0^2 . \quad (21)$$

The resonance condition at ω_0 may be determined by measuring the power transmitted through a resonating system such as described previously. This may be done at a constant discharge current by varying the frequency and noting the frequency at which the transmitted power is a minimum. This method, however, is very cumbersome because the resonating system and associated coaxial cable must be tuned for each frequency so as to provide a maximum E field at the discharge tube.

Also, if the signal generator output varies with frequency, another adjustment is necessary. It is more convenient to vary the current at a fixed frequency and to note the current for minimum transmitted power. The experimental equipment described in the next section provides the means for displaying the transmitted power on an oscilloscope as a function of discharge tube current. The resonance condition, the current for resonance, and the resonant frequency are thus conveniently obtained.

4. Equipment

Fig. 3 is a photograph of the experimental equipment arrangement.

The equipment used can be grouped into six general classes:

1. Vacuum system
2. Pressure measuring equipment
3. Discharge tube
4. D. C. circuitry
5. Current modulator
6. R. F. circuitry

Vacuum System

The vacuum was provided by a Consolidated three stage water-cooled diffusion pump and a Welsh Duo-Seal mechanical fore-pump. Octoil-S was used as the pumping fluid in the diffusion pump. The ultimate vacuum attained was 2.0×10^{-7} mm Hg. The entire system down to the diffusion pump was baked for several hours at approximately 300°C by means of heating tapes heavily lagged with asbestos cloth. The vacuum system was separated into two parts and mounted on separate tables. On one table were the pumps and on the other the discharge tube, oil manometer, gas bottles of neon and argon, and the vacuum gauges. The two tables were separated by a liquid air trap. Glass stopcocks were lubricated with Apiezon Type-N grease.

Pressure Measuring Equipment

Pressures in the high vacuum range, 10^{-4} to 10^{-7} mm Hg, were measured with a Carl Herrmann Associates, Bayard-Alpert type, IG-100

ion gauge tube controlled by a Veeco RG 31A Vacuum Gauge.

Pressures in the range 10^{-1} to 10^{-3} mm Hg were measured by a Westinghouse Type 7903 ion gauge tube. The 7903 tube was calibrated with an oil manometer as follows. The ratio of volumes of the oil manometer alone to the volume of the entire system including the discharge tube, manometer and connecting glass piping was measured. This was accomplished by filling the manometer with gas near the extreme of its capacity, sealing it off and evacuating the rest of the system, then allowing the gas in the manometer to flow into the system. The two readings of manometer displacement gave the volume ratio. With this ratio an easily readable height of oil in the manometer was converted to pressures in the range 10^{-3} to 10^{-1} mm Hg using the formula:

$$\text{Pressure mm Hg} = Y \text{ cm oil} \times \frac{.672 \text{ mm Hg}}{\text{cm oil}} \times \text{Ratio} \frac{\text{Vol. manometer}}{\text{Vol. system}}$$

For example, 1 cm oil corresponded to 7.3×10^{-3} mm Hg with Discharge Tube I on the system. The oil manometer was read with a Gaertner Cathetometer at a distance of approximately 10 feet. The manometer and cathetometer determined the pressure to less than 5% error. The Westinghouse 7903 ion gauge was then calibrated from the manometer readings. Details of the 7903 ion gauge and the calibration curves are given in the appendix.

Discharge Tube

Two similar discharge tubes, labeled Tube I and Tube II, were used in this work. The tube dimensions are given in Fig. 4. Both were of the hot cathode type using a coiled ribbon, oxide coated tungsten filament, Westinghouse Style No. 14-39601, rated at 5 volts, 7.5 amperes. The filament was supported inside a tantalum cylinder left open at both ends. The cylindrical shield was left "floating" electrically and was completely successful in preventing filament material deposit on the tube walls as far as the eye could tell.

The anode for both tubes was a tantalum disk spot-welded to a single tungsten rod support. The edge of the round disk was spun over to form a shallow cup opening away from the cathode.

The glass envelopes were locally constructed from pyrex tubing.

D. C. Circuitry

The experimental circuitry is shown in Fig. 5. The filament power was supplied by a Perkin MR 532-15, magnetic amplifier regulated, d. c. power supply with a 15 ampere capacity. This power supply was found to have excessive ripple so two filter sections each consisting of a 10 henry choke and a 2000 microfarad capacitor were added. It was necessary to keep the filament above ground in order to sample the discharge tube current waveform across the 10 ohm resistor R-1 so the filament power supply was fed through an isolating transformer. The discharge tube plate power supply was a locally manufactured 2 kilovolt-500 milliamperes unregulated power supply.

Current Modulator

As mentioned in the Introduction, in determining a resonance condition, it is more practical to use a fixed frequency and sweep the current than vice-versa. To provide a current sweep several methods were attempted.

First, the secondary of a one to one transformer was connected in series with the discharge tube and a 60 cycle voltage from a Variac impressed on the primary. This provided a satisfactory current sweep amplitude but the d.c. current passing through the transformer secondary raised the operating point of the transformer up to near the knee of the magnetization curve. This resulted in a hysteresis effect and a double trace on the oscilloscope. Larger transformers with up to 6 KVA capacity were tried but insufficient improvement was noted.

To eliminate this hysteresis effect, current modulation by electronic means was attempted. Due to the high d.c. discharge tube current (up to 500 milliamperes), it was impractical to put a commonly available electronic tube in series with the discharge tube so a circuit was devised to place a variable electronic load in parallel with it. This provided a satisfactory current sweep, but it also provided an additional path to ground for the discharge tube noise. The discharge tube noise was enhanced by a factor of four and completely masked the resonance condition displayed on the oscilloscope.

A satisfactory current sweep was attained with the construction of the Current Modulator shown in Fig. 6. This modulator uses the sawtooth

voltage waveform provided by the Tektronics 555 Dual-Beam Oscilloscope as its input. Since the entire current modulation circuit is off ground, it was necessary to couple the input through an isolating transformer. The resistor R-5 is provided to help couple the high impedance oscilloscope sawtooth output to the much lower transformer impedance. This coupling was not entirely satisfactory, resulting in a very slight distortion of the sawtooth waveform. A suggested improvement is to add a cathode follower stage for coupling to the high impedance oscilloscope sawtooth output. The potentiometer R-4 controls the modulation amplitude and the potentiometer R-3 provides a variable bias. Both these controls are necessary to provide an undistorted current sweep over the range of 10 milliamperes to 500 milliamperes discharge tube current.

The discharge tube current waveform was monitored continuously during the measurements by displaying the voltage across the 10 ohm resistor R-1 on the lower trace of the dual-beam oscilloscope. This voltage also provided the sweep for the upper trace by connection to the external horizontal plates. It was necessary to couple to the external horizontal plates through the large capacitor C-1 (Fig. 5) because the d.c. voltage across R-1 exceeded the horizontal positioning control of the oscilloscope. The calibration of the lower trace vertical amplifier gave a convenient measure of the upper trace horizontal sweep amplitude.

Through trial and error it was found that a 400 cps sweep rate was optimum. Too slow a sweep repetition rate resulted in a hysteresis effect (double trace) much like that encountered with transformer modulation. Possibly this was caused by ion bombardment changing the cathode temperature during the cycle. Too fast a sweep rate exceeded the response capability of the circuit.

R. F. Circuitry

R. F. power was provided with a Hewlett Packard Model 608C VHF Signal Generator. Coaxial cable RG-59 was used throughout the R. F. circuit. The signal from the generator was connected to one side of a strip-line assembly, Fig. 7, which enclosed the discharge tube. From the other side of the strip-line, connection was made to a General Radio 50cm Adjustable Line and a 50cm Adjustable Stub connected together. After these tuning elements came the detector consisting of a Sylvania 1N26 crystal held in a Hewlett Packard Model 420A Crystal holder shunted with a .47 microfarad capacitor (Fig. 5). The detector output was connected to the vertical input of the upper trace on the Tektronics 555 Oscilloscope. The horizontal sweep for this trace was provided by the sawtooth current waveform, through the external horizontal amplifier.

Strip-line Assembly. The ideal resonating system of Fig. 2 was approximated with a strip-line assembly shown in Fig. 7. The strip-line was constructed of copper sheet with the two sides separated by a dielectric spacer of one-half inch plexiglass. Overall length was 20 centimeters. Electrical connection was by BNC connectors soldered

to one side with the center wire led through the spacer to the other side. Two strip-lines were used, identical except for the diameter of the circular portion. These diameters are given in Table 2. This strip-line was virtually identical to the Type II used by Crawford, et al,⁶ who performed a series of experiments to determine the effects of metal to glass spacing, strip-line width and eccentricity of tube position. They found that the effect of reducing the strip-line width was to lower the current for resonance.

The width of the strip-lines used in this work was 1.6 cm and it is estimated that the densities measured may be 20% too low.⁶ It was not practical to increase the widths used because of longitudinal density gradients in the discharge tubes.

It was found that standing striations existed in both discharge tubes at virtually all currents and gas pressures used. These striations were usually quite visible near the cathode and were commonly spaced about 4 centimeters apart. The strip-line was easily able to resolve the density difference between a striation and the darker area on either side. Near the cathode the electron number density of the striation was roughly 30% to 60% greater than the density of the adjoining dark area. Although not usually visible, these striations were often present throughout the positive column as determined by the strip-line.

Since the strip-line resonant frequency is determined by the electron number density, density gradients have the effect of lowering the effective Q of the resonant system. The Q of this system was

marginal at high gas pressures and the lower effective Q from a wider strip-line could not be accepted.

In this type of resonating system it is common to observe a main resonance and one or more subsidiary resonances at both higher and lower frequencies than the main resonance. The explanation for these subsidiary resonances is controversial, but the resonances occurring at higher currents than the main resonance are often attributed to higher order azimuthal modes. It is commonly accepted that the main resonance is due to the $m = 1$ or dipole mode as shown in Fig. 2b. In this work, the main resonance alone was usually observed. An oscillogram of a typical resonance is shown in Fig. 8. The resonance peak is inverted because the crystal detector supplies a negative signal. The lower trace is the current wave-form which supplies the horizontal sweep for the upper resonance trace.

The failure to routinely observe the expected subsidiary resonance (not a discouraging result since they are quite troublesome) could be due to many factors. Chief among them is the high noise level of the system as seen on the rather blurred trace of Fig. 8. Herlofson⁸ has pointed out that collision damping is more serious for modes of higher order. This was borne out in that the one clear observation of a subsidiary resonance, shown in Fig. 9, occurred in argon at a very low pressure. In Fig. 9, the main resonance peak is on the left at 220 milliamperes, and the subsidiary resonance peak is on the right at 278 milliamperes. Note that on Fig. 9, and on all

oscillograms, "Discharge current" or "Current" refers to the average discharge current and its value fixes the centerpoint of the upper trace horizontal sweep. Also, the metal shorting rings, which enclose the tube on either side of the strip-line proper (see Fig. 7) have the effect, when properly spaced, of emphasizing the main resonance.⁶ This effect was quite small, but at high pressures where the Q was marginal any increase in the apparent Q was welcome.

In order to determine n_0 , the electron density on the axis of the tube, a knowledge of the radial variation of the electron density, giving the value of α in equation (14), is necessary. This must be determined by means other than discussed here, such as radial probe measurements. A knowledge of this parameter was not at hand and accordingly the results quoted will pertain only to the mean electron number density \bar{n}_e , which just requires evaluation of the constant k_1 . Table 1 below gives the values of k_1 calculated from equation (16).

	Discharge Tube Diameter		Strip-line Diameter	k_1
	I.D. (=2a)	O.D. (=2b)	I. D. (=2c)	
Tube I	3.75 cm	4.16 cm	5.00 cm	6.29
Tube II	3.11 cm	3.51 cm	4.71 cm	4.73

Table 1. The constant k_1

With these values of k_1 , the mean electron number density \bar{n}_e is determined from equation (17b). Table 2 lists values of mean electron number density for various resonant frequencies in the range covered.

Resonant Frequency- f_0	Number Density - \bar{n}_e	
	Tube I	Tube II
100 mc/s	$7.8 \times 10^8 / \text{cm}^3$	$5.9 \times 10^8 / \text{cm}^3$
200 mc/s	$3.1 \times 10^9 / \text{cm}^3$	$2.3 \times 10^9 / \text{cm}^3$
300 mc/s	$7.0 \times 10^9 / \text{cm}^3$	$5.3 \times 10^9 / \text{cm}^3$
400 mc/s	$1.2 \times 10^{10} / \text{cm}^3$	$9.4 \times 10^9 / \text{cm}^3$
480 mc/s	$1.8 \times 10^{10} / \text{cm}^3$	$1.3 \times 10^{10} / \text{cm}^3$

Table 2. Electron number densities

5. Procedures

The data presented in the section on Results were obtained by determination of the discharge current value required for resonance at resonant frequencies, f_0 , from 100 to 480 megacycles and at various gas pressures. After thorough evacuation, the system was filled with gas (neon or argon) to a specified pressure as measured by the manometer and cathetometer. The discharge was then ignited and the pressure monitored with the Westinghouse 7903 ion gauge. At a fixed frequency f_0 , the current required for resonance was then determined by varying the power supply output until the resonance was displayed on the oscilloscope. The 50 cm adjustable line and 50 cm adjustable stub were positioned as necessary to give a peak response. The current modulator bias and modulation amplitude controls were also manipulated as required to provide an undistorted current sweep and adequate sweep amplitude. At each frequency, the frequency f_0 , the average discharge current I , the tube voltage drop from anode to cathode, and the pressure were recorded. These readings were taken at 20 megacycle intervals over the range 100 to 480 megacycles or until a maximum current of 500 millamperes was attained. The system was then evacuated, a new quantity of gas introduced, and the process repeated.

Data were obtained for only one strip-line position on each tube. This position was chosen to be in the positive column relatively far from the cathode and the intense standing striations there. On Tube I the position was 21.5 centimeters from the anode and on the longer

Tube II, 33.5 centimeters from the anode.

Criteria for resonance. The establishment of a criterion for determination of the current value for resonance is a difficult problem. The response viewed on the oscilloscope is inherently asymmetrical because of the electron density variation. At the high current (high density) end of the sweep the increased electron density affords opportunity for greater power absorption. Also, unseen (because of noise) subsidiary resonances may distort the response. For these reasons the criterion of maximum amplitude is suspect. The criterion adopted in this work was the obtaining of the most symmetrical resonance curve. In cases of doubt, the low current side was favored. Figs. 10 and 11 illustrate this criterion and give an indication of the precision with which the current for resonance may be determined. The lower current side of the response, in general, was steeper in that the response amplitude fell off more rapidly as the current was reduced from resonance than if it was increased from resonance.

On the oscillograms, it should be noted that the end to end value of the current sweep providing the abscissa of the upper trace can be determined directly from the lower trace showing the current waveform. For example, in Fig. 10a the height of the lower trace is 0.8 centimeters and the sensitivity is 50 milliamperes per centimeter so the upper trace horizontal width corresponds to 40 milliamperes.

As predicted from the expression for the theoretical Q of the strip-line,

$$Q = \frac{\omega_0}{\gamma} \quad (18)$$

the pressure has a marked effect on the resonant response. An increase in pressure increases the collision frequency and results in a degradation of the Q. This is illustrated in Fig. 12 showing 3 resonances in neon at nearly equal current but different pressures. The upper trace sensitivity should be noted to permit comparison.

The magnitude of the average current also affected the resonance although not so markedly as pressure. The chief effect of increasing current was to increase the noise level. This is illustrated in Fig. 13 showing two resonances in neon at the same pressure but different currents. The increased current sweep amplitude in (b) was required to determine the resonance point.

6. Results and Discussion

Shown in Fig. 14 is a log-log plot of current for resonance vs $1/p$ (inverse pressure) at resonant frequencies from 120 to 480 megacycles for an argon plasma in Tube I. Fig. 15 shows the same plot for neon in Tube I and Fig. 16 is this plot for argon in Tube II. Neon was not investigated in Tube II. It was necessary to plot the data in this form in order to obtain the resonant frequency characteristics at constant pressures, since the pressure proved to be a function of current. This effect is discussed later under Clean-up. The parameter $1/p$ was chosen as the most meaningful parameter available in terms of functional dependence. From equation (19), $I = \bar{n}_e A e \bar{v}$, and since specifying the resonant frequency f_0 determines \bar{n}_e , it is seen that the plots of Figs. 14-16 have the same form as a plot of \bar{v} vs $1/p$. Now \bar{v} is a function of E/p and although the value of the field E in the positive column was not available, it is expected to be approximately constant over a wide range of current in a normal glow discharge. It is regretted that provision was not made to measure E in the column near the strip-line.

To obtain a rough estimate of the value of E in the positive column, the average electron velocity was calculated for argon in Tube I at a pressure of 4.7×10^{-2} mm Hg. At a current of 100 milliamperes and a resonant frequency of 425 megacycles, the average electron velocity was calculated to be 4×10^6 cm/sec. Published curves of v vs E/p do not extend to this high a value of electron velocity, but Neilsen⁹ provides a curve that can be extrapolated and a value of $E/p = 11$ was

obtained. Comparison with the pressure of 4.7×10^{-2} mm Hg yields a value of 0.5 volts/cm for E . Using this value, the positive column would account for 30% of the total anode to cathode voltage drop, an entirely reasonable result. The same calculation was made for neon in Tube I at 7.3×10^{-1} mm Hg. At a current of 100 milliamperes and resonant frequency of 405 megacycles, the average electron velocity was calculated to be 4.4×10^6 cm/sec. Another extrapolation¹⁰ yielded the unreasonable result of $E = 5$ volts/cm. Using this value, the voltage drop in the positive column would be over twice that recorded for the entire tube. The extrapolation necessary for this calculation was quite gross and this unreasonable result suggests that the indicated curve of v vs E/p does not hold at high velocities, probably due to excitation. The behavior of v vs E/p at high v could be conveniently determined if the methods of this work were combined with a measurement of E in the positive column.

Fig. 17 shows a log-log plot of current for resonance vs resonant frequency at various pressures for an argon plasma in Tube I. Fig. 18 shows the same plot for neon in Tube I and Fig. 19 is for argon in Tube II. A straight line of slope 2 was drawn through the data points for each pressure. The adherence or non-adherence of the points to these lines give a measure of the validity of the assumption of equation (20), $I \sim \bar{n}_e$. It is seen that, in general, there was a deviation from these lines at high current. The deviations were on the high current side in all cases. This is the side where the deviation would be expected if

E had increased at high current. It was, in fact, noted that the anode to cathode voltage drop did increase slightly at the higher current values and it is reasonable that E would take the same direction. It is believed that had the current I been plotted vs E/p (Figs. 14-16), much closer adherence to the lines of slope 2 (Figs. 16-19) would have resulted.

Comparison of Figs. 17 and 18 shows that at equal electron density and gas pressure the current in neon was much higher. This is expected since argon is subject to the Ramsauer effect while neon is not. And, in general, argon has a higher collision cross-section for electrons.

Comparison of Figs. 17 and 19 shows a higher current for Tube I at equal pressure and density as expected from its larger diameter.

It was noted that at equal pressures the resonant curve was much sharper (higher Q) in Tube II than in Tube I. This effect is illustrated by comparison of Figs. 10 and 11 where it is seen that the resonance of Fig. 11 (Tube II) is markedly sharper even though at a slightly higher pressure. This effect of decrease in Q with increase in tube diameter was previously reported by Dattner⁵ in a resonant system employing waveguides.

Of especial interest is the pressure range over which resonance was obtained. In argon, the upper limit was approximately 5×10^{-2} mm Hg. Above this pressure the Q was too low to permit a determination of resonance. In neon, quite good resonances were obtained at 7.3×10^{-1} mm Hg. This large pressure range suggests that this method of electron density measurement should find good applicability in neon.

The lower limit of pressure in both gases was determined solely by the inability to maintain a normal glow discharge. At approximately 1×10^{-3} mm Hg the argon discharge shifted to an abnormal mode, here termed a "collapsed discharge". This collapsed discharge was characterized by its high impedance and a long dark space next to the cathode. In neon the same effect occurred at approximately 1×10^{-2} mm Hg. Fig. 20 shows a V - I characteristic taken with Tube I filled with neon at 1.2×10^{-2} mm Hg. The normal glow characteristic was taken immediately after igniting the discharge. As the current was increased to above 300 milliamperes the pressure decreased to below 1×10^{-2} mm Hg, whereupon the discharge suddenly shifted to the collapsed discharge characteristic. The voltage then decreased and the discharge returned to the normal characteristic. In this manner the discharge would oscillate between the two characteristics with a period from one to several seconds. After some time, the discharge shifted completely to the collapsed characteristic where it remained. The collapsed discharge characteristic on Fig. 20 was obtained after this occurred. This effect was observed many times in both argon and neon. It was observed that when the tube was newly installed on the system, the onset of this effect occurred at a higher pressure in both gases. After operating a discharge and then evacuating the system several times, the onset of the effect stabilized at 1×10^{-2} mm Hg in neon. This suggests that the effect is due to the impurity content of the gas as well as pressure. Alderson and Leonard¹¹ reported this effect in neon, at similar pressures, using a tube of

different construction.

It was sometimes possible to arrest the transition to the collapsed mode by lowering the discharge current. The tube would then operate on a $V - I$ curve between the two shown in Fig. 20, so long as a critical current was not exceeded and the pressure remained constant. The discharge under these conditions was remarkable for its low noise. A search for the resonance response under these conditions in argon at 1.5×10^{-3} mm Hg produced the unusual series of very sharp peaks shown in Fig. 21. The orderly series of resonances on the high current side of the main resonance is reminiscent of the series of resonances reported by Dattner⁵ on the low current side of the main resonance. The conditions necessary for this response were impossible to reproduce with any accuracy and this effect was not further investigated. It may well be that the resonance curve for the normal glow discharge also consists of this series of sharp resonances, but due to the high noise level only the envelope is detected.

Clean-up effects. As mentioned previously, it was found that the pressure in the system varied with the discharge current. Fig. 22 shows this variation in Tube I with argon. The tube had been thoroughly evacuated and filled to a pressure of 1×10^{-2} mm Hg. The discharge was then ignited and the current was raised in small steps to 500 milliamperes and then reduced, also in small steps. At lower pressures the original variation was even more marked and the recovery less when the current was subsequently reduced. At pressures above 2×10^{-2} mm Hg the

variation was not significant although some reduction in pressure occurred when the discharge was first ignited. The same form of variation was observed in both gases although not to the same extent in neon since discharges could not be maintained below 1×10^{-2} mm Hg.

Dushman¹² extensively discusses this effect which he terms "clean-up". It was concluded¹³, that in hot cathode discharges, clean-up occurs by penetration of ions possessing considerable kinetic energy into the walls.

In this work, to reduce measurement errors due to changing pressure, it was found prudent to commence measurements at high current and work downward. The procedure did not eliminate the pressure variation with current (see Fig. 22), but substantially reduced it especially at the lower pressures.

7. Recommendations

The following areas are recommended for further investigation:

- a. Investigate the standing striations encountered in this work.

Measurements of electron number density by the strip-line method could be correlated with measurements of the light output along the column.

- b. Determine the behavior of v vs E/p at high velocities, where there is a lack of information in the literature. This would require measurement of E in the positive column. The use of a movable anode is suggested for this measurement.

- c. Correlate the number densities measured by the strip-line method with probe measurements in various gases. Radial probe measurements would also determine the radial density variation. Measurement of the electron temperature would permit correlation between the electron mean free path and the upper pressure limit of the strip-line method in various gases.

- d. Investigate the resonance behavior in the presence of magnetic fields.

- e. Endeavor to reduce the noise generated in the discharge tube in order to improve measurement accuracy.

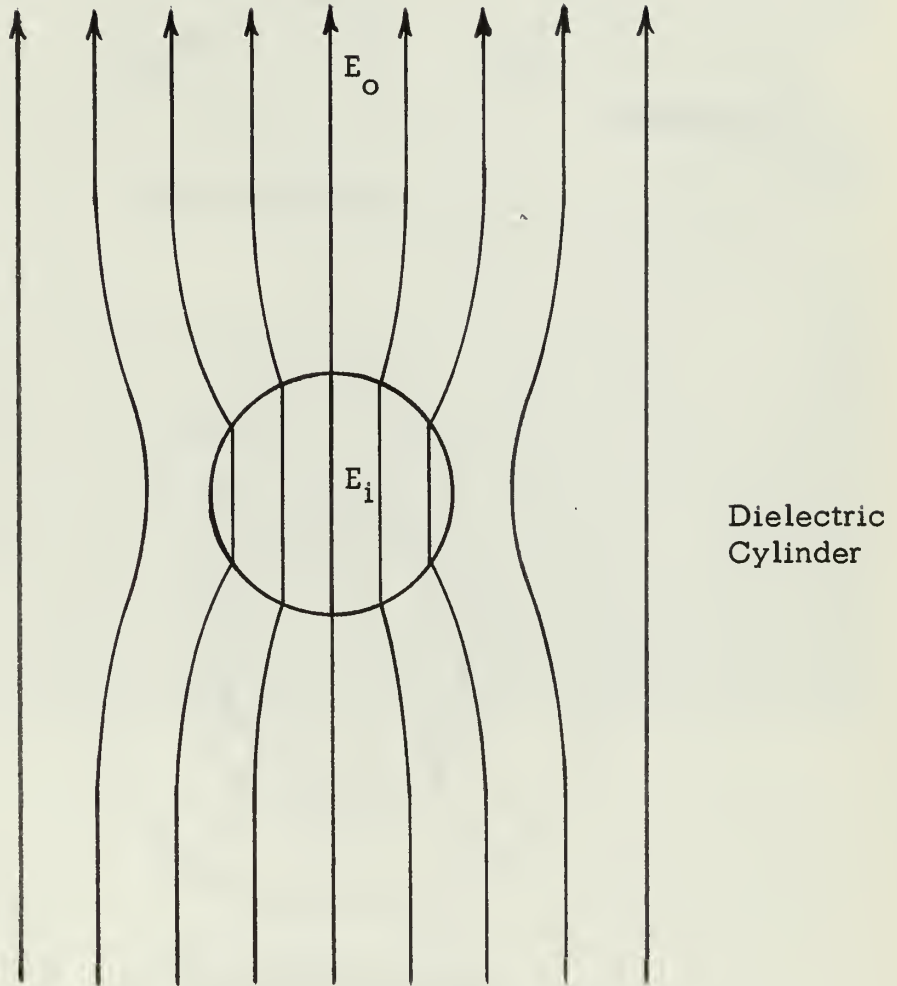


Fig. 1. Dielectric cylinder in an uniform electric field

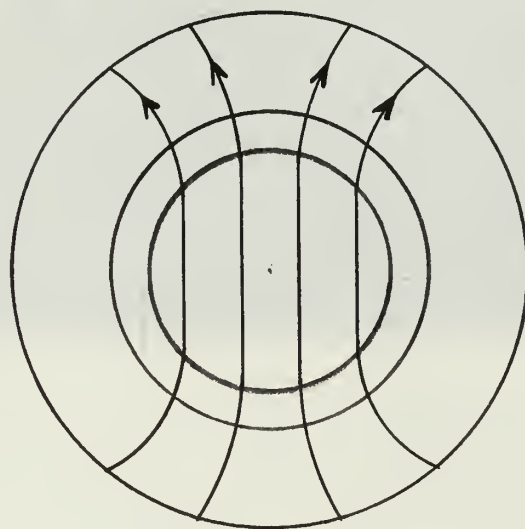
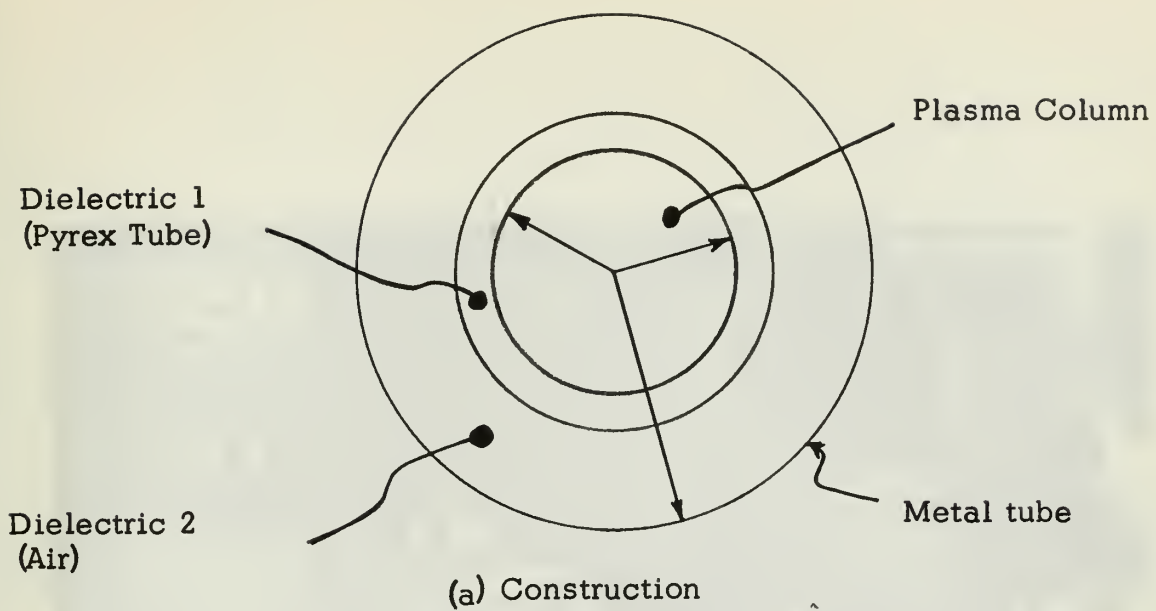


Fig. 2. Ideal resonating system

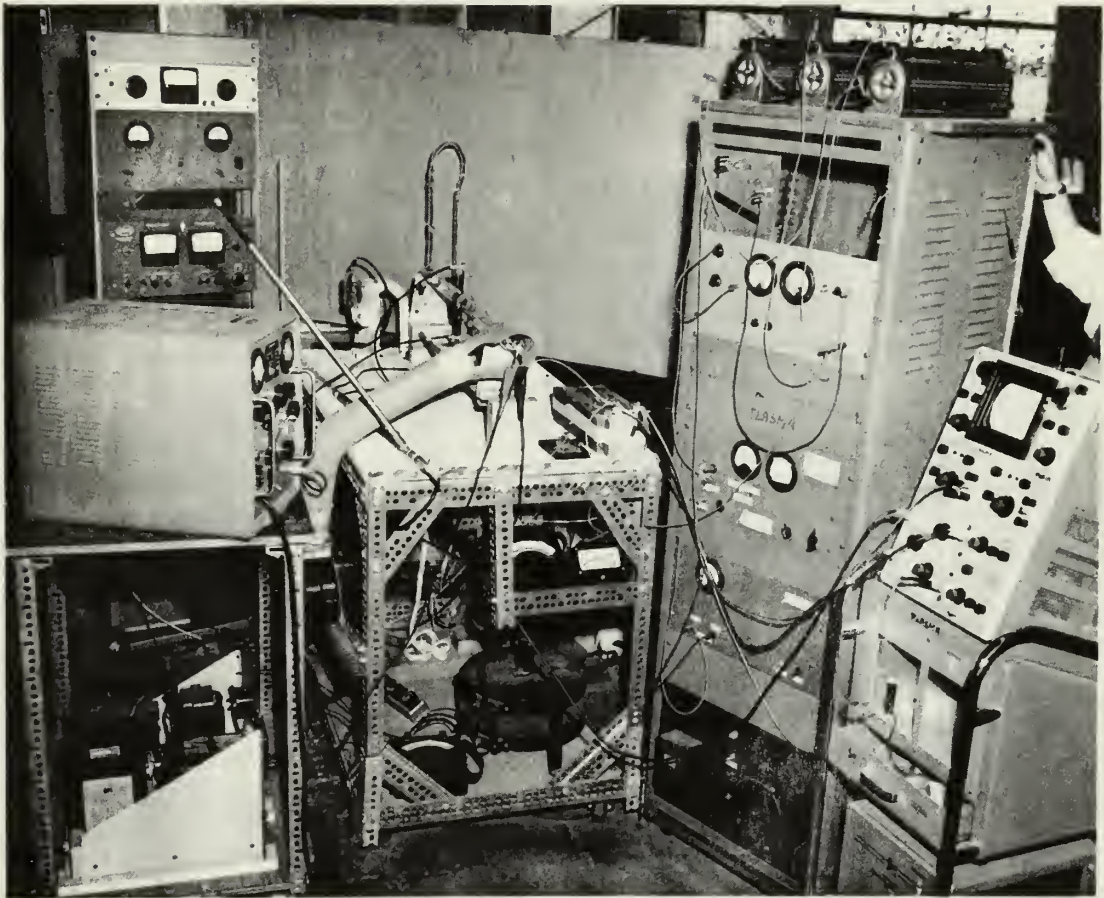
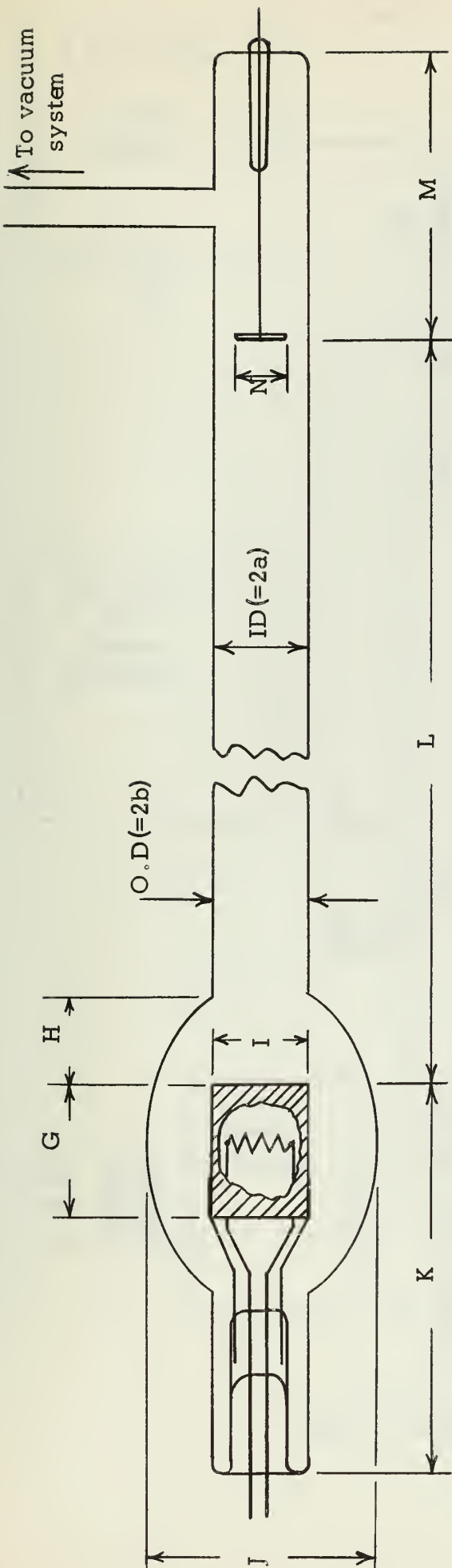


Fig. 3. Experimental equipment arrangement



Tube No.	Dimensions in centimeters										
	ID(=2a)	OD(=2b)	G	H	I	J	K	L	M	N	
I	3.75	4.16	3.10	3.0	3.20	6.6	10.5	58.7	13.0	3.18	
II	3.11	3.51	2.64	2.0	2.43	5.0	11.8	74.3	14.1	1.90	

Fig. 4. Experimental Discharge Tube

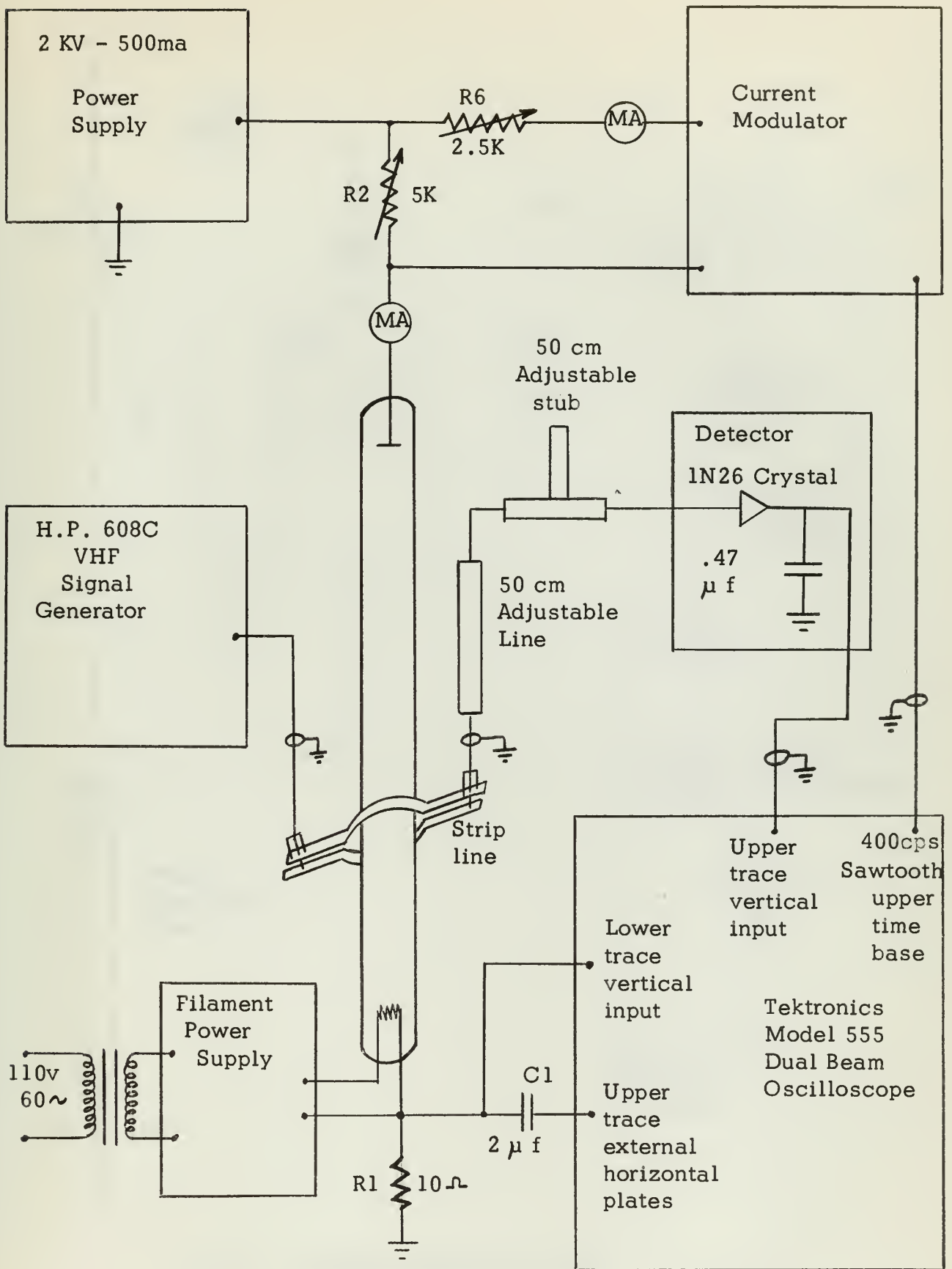


Fig. 5. Experimental circuitry

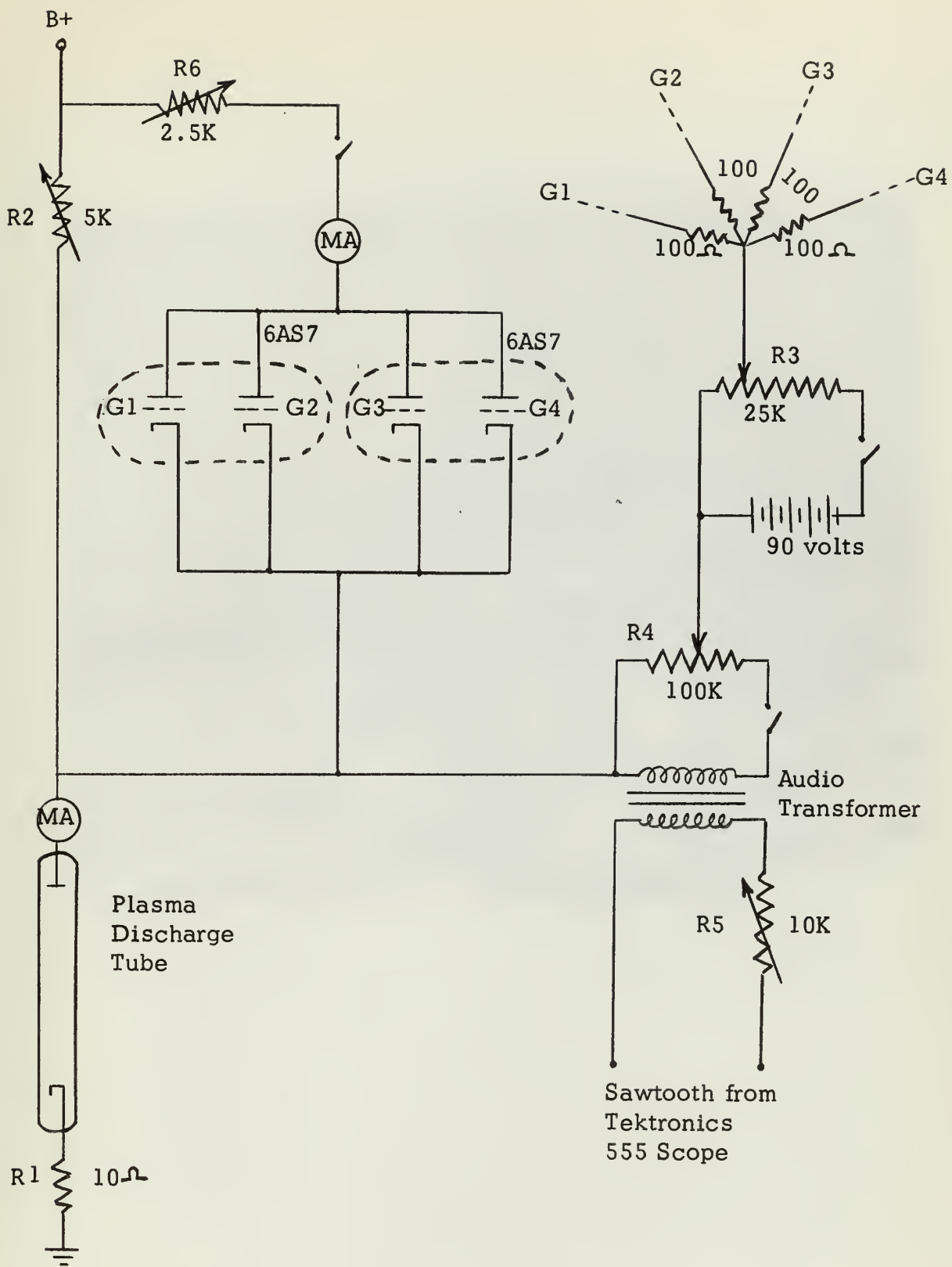


Fig. 6. Current modulation circuit

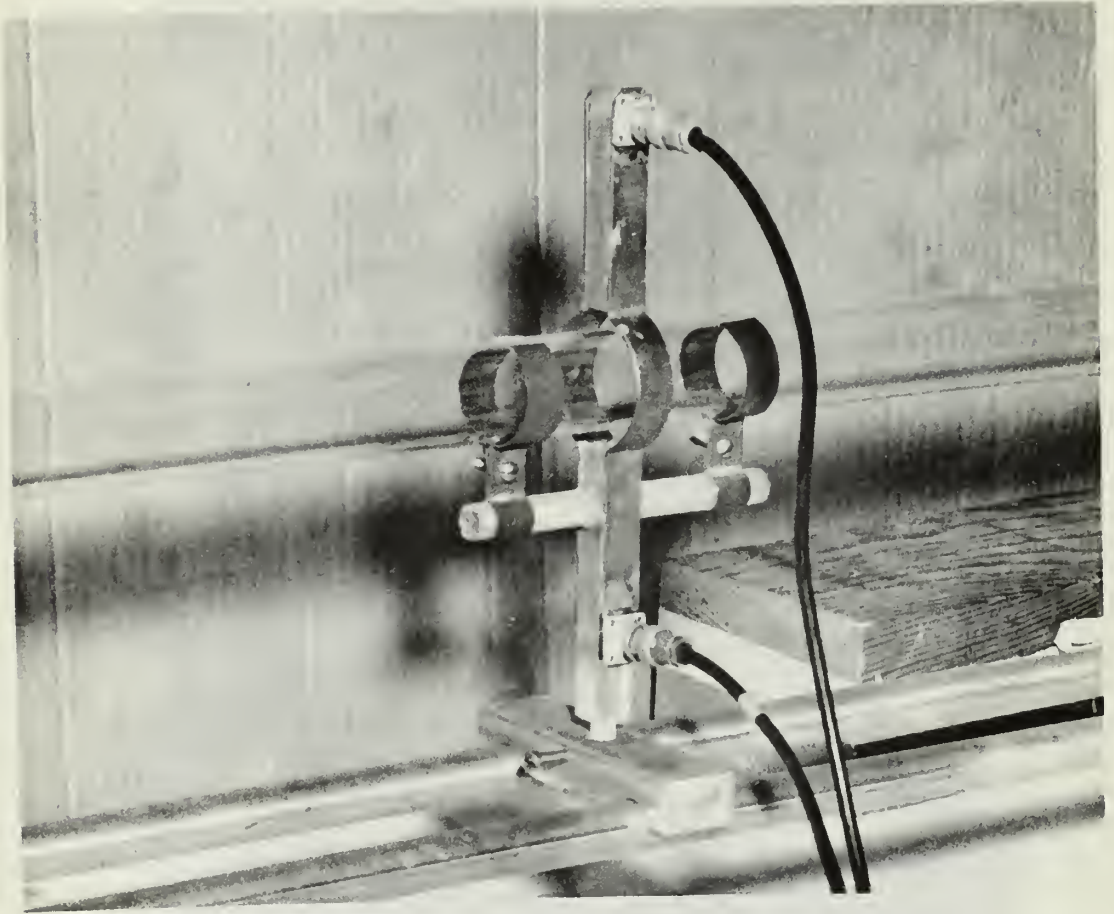
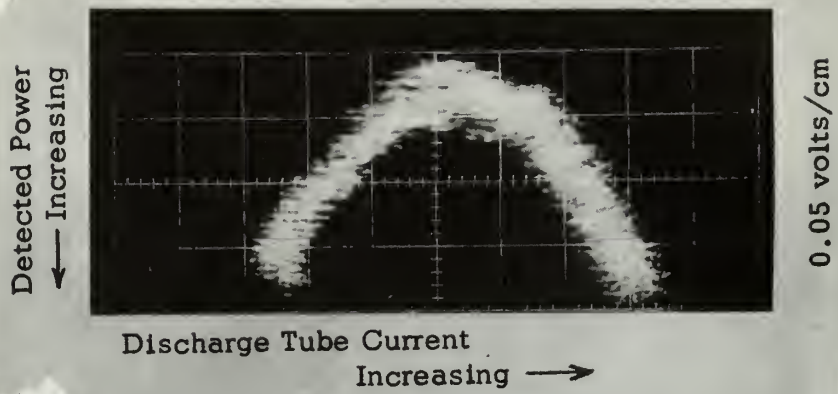


Fig. 7. Strip-line assembly

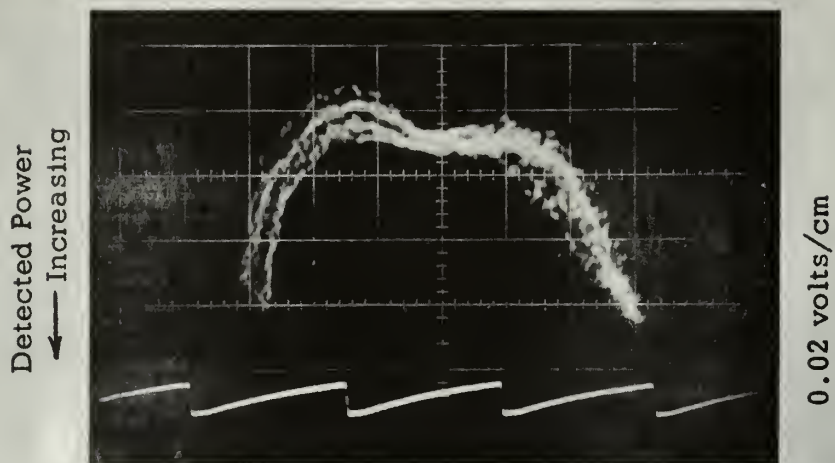


(a) Oscillogram of plasma resonance



(b) Discharge current waveform

Fig. 8. Oscillogram of typical resonance condition



Discharge Tube Current
Increasing →

Tube II (Inside Diameter = 3.75 cm)

Gas - Argon

Pressure - 3.0×10^{-3} mm Hg

Resonance Frequency - $f_0 = 320$ mc/s

Discharge Current - 250 ma

Resonance peaks at 220 ma and 278 ma

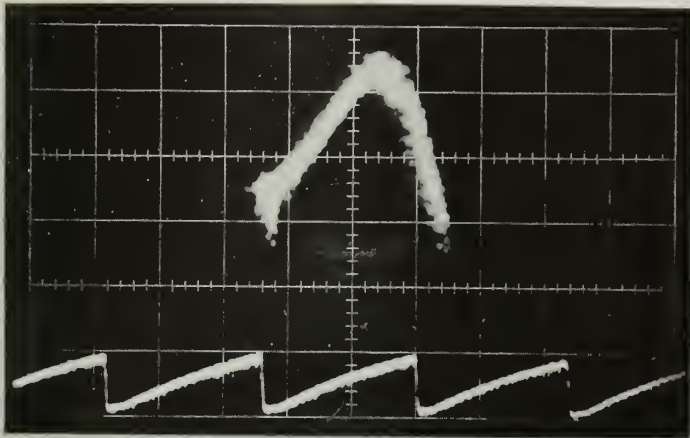
Lower Trace

Current waveform

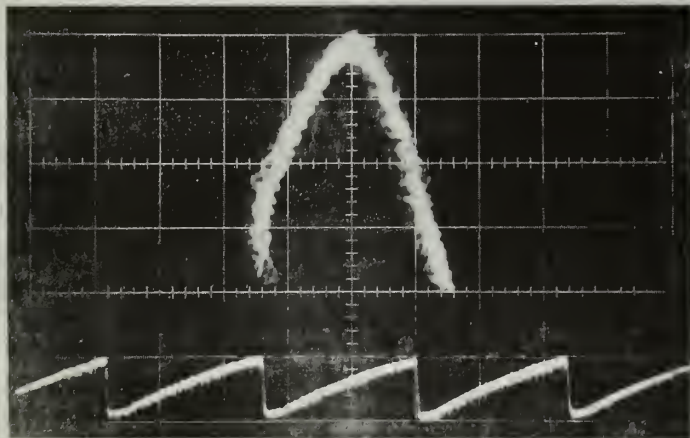
100 ma/cm

400 cps

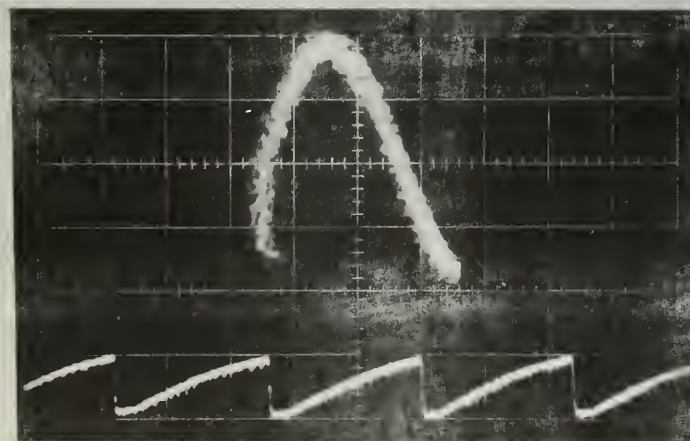
Fig. 9. Subsidiary Resonance



(a) Below resonance ($I=93$ ma)



(b) At resonance ($I=102$ ma)



(c) Above resonance ($I=113$ ma)

Tube I
(Inside Diameter = 3.75 cm)

Gas - Argon

Pressure - 1.6×10^{-3} mm Hg

Resonant Frequency
 $f_0 = 160$ mc/s

Upper Trace

Vertical - Detected Power ↓
.02 volts/cm

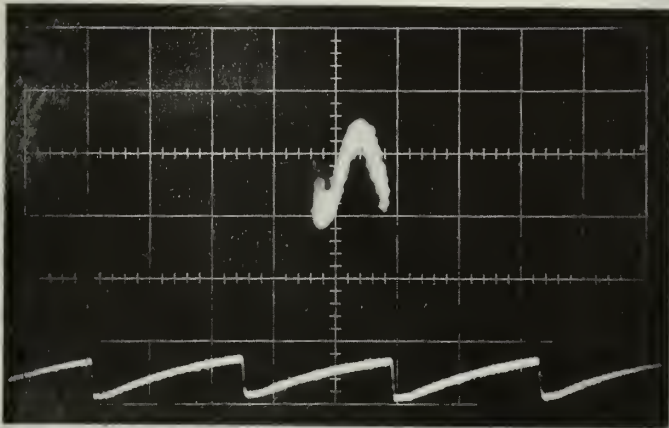
Horizontal - Current
Increasing →

Lower Trace

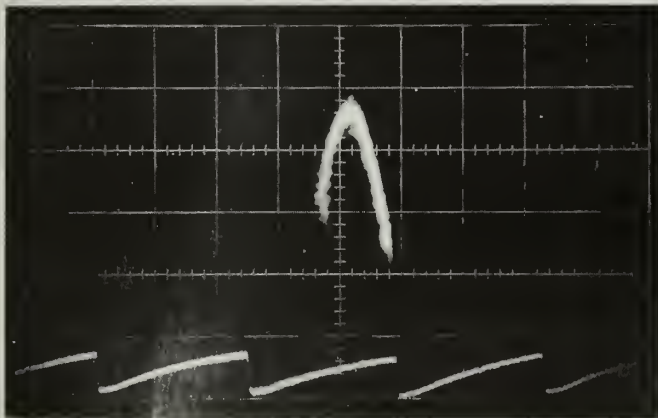
Vertical - Current
50 ma/cm

Horizontal - Time
400 cps

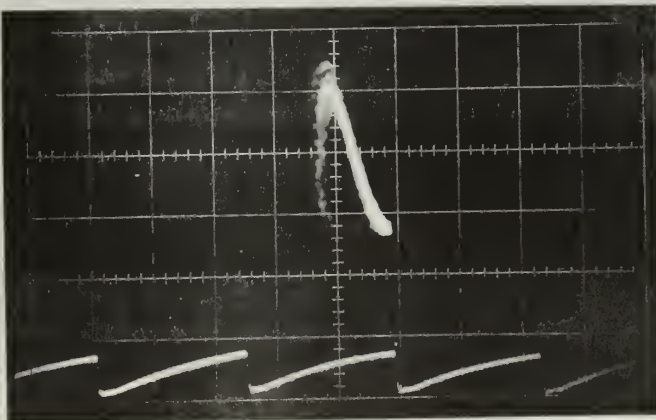
Fig. 10. Resonance in Tube I



(a) Below Resonance ($I=55$ ma)



(b) At Resonance ($I=60$ ma)



(c) Above Resonance ($I=70$ ma)

Tube II
(Inside Diameter = 3.11 cm)

Gas - Argon

Pressure - 3.4×10^{-3} mm Hg

Resonance Frequency
 $f_0 = 180$ mc/s

Upper Trace

Vertical - Detected Power
0.01 v/cm

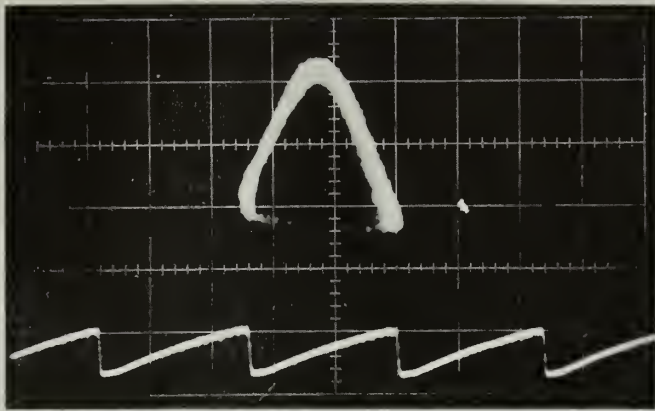
Horizontal - Current
Increasing \rightarrow

Lower Trace

Vertical - Current
20 ma/cm

Horizontal - Time
400 cps

Fig. 11. Resonance in Tube II



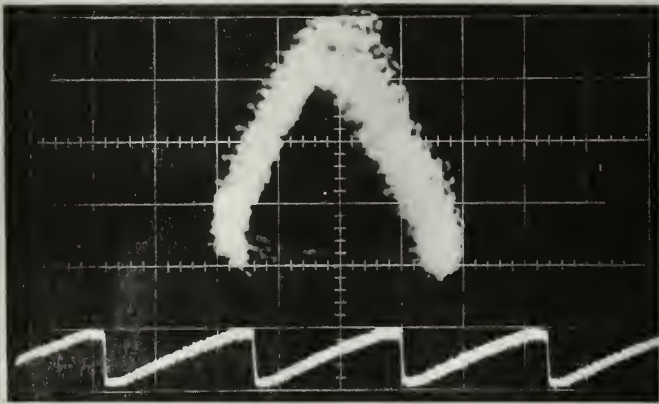
(a) Pressure 1.7×10^{-2} mm Hg

$$f_0 = 120 \text{ mc/s}$$

$$I = 50 \text{ ma}$$

Upper Trace
Detected Power ↓
0.01 volts/cm

Lower Trace
Current →
50 ma/cm
400 cps



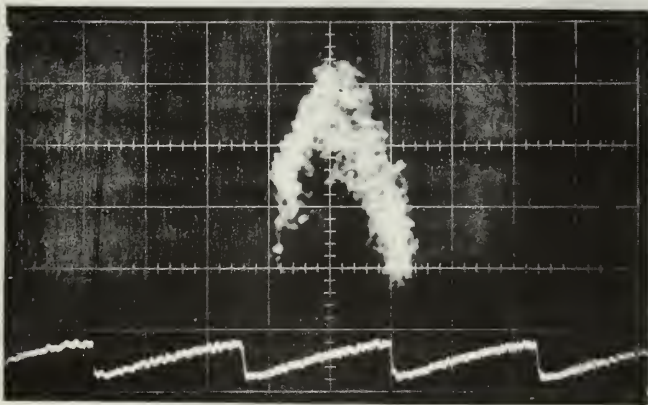
(b) Pressure = 7.0×10^{-2} mm Hg

$$f_0 = 220 \text{ mc/s}$$

$$I = 65 \text{ ma}$$

Upper Trace
Detected Power ↓
0.005 volts/cm

Lower Trace
Current →
50 ma/cm
400 cps



(c) Pressure = 2.1×10^{-1} mm Hg

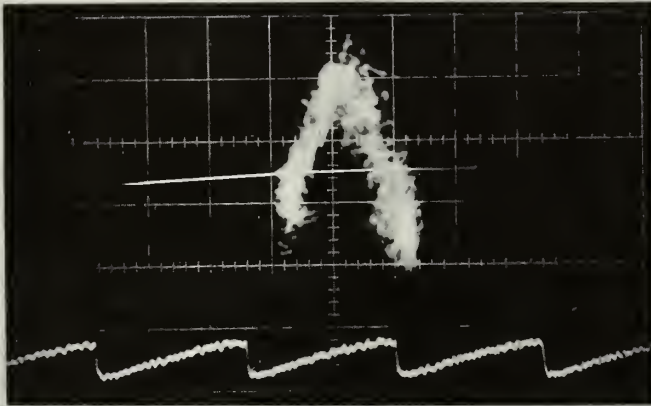
$$f_0 = 260 \text{ mc/s}$$

$$I = 55 \text{ ma}$$

Upper Trace
Detected Power ↓
0.005 volts/cm

Lower Trace
Current →
50 ma/cm
400 cps

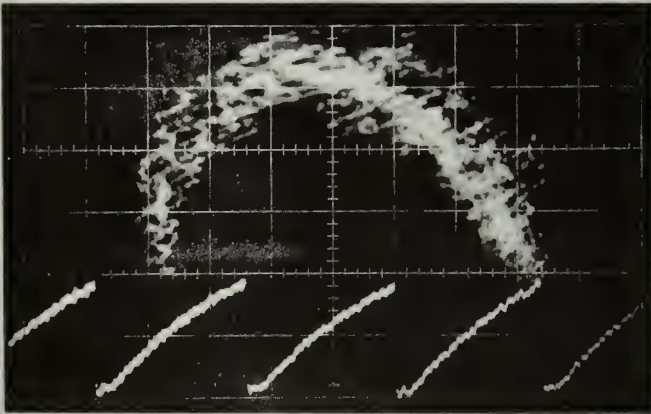
Fig. 12. Effect of pressure on Resonance in Tube I with neon.



(a) Discharge Current = 55 ma
 $f_0 = 260 \text{ mc/s}$

Upper Trace
 Detected Power ↓
 0.005 volts/cm

Lower Trace
 Current Waveform
 50 ma/cm
 400 cps



(b) Discharge Current = 240 ma
 $f_0 = 480 \text{ mc/s}$

Fig. 13. Effect of discharge current on resonance in Tube I with neon at pressure of $2.1 \times 10^{-1} \text{ mm Hg}$.

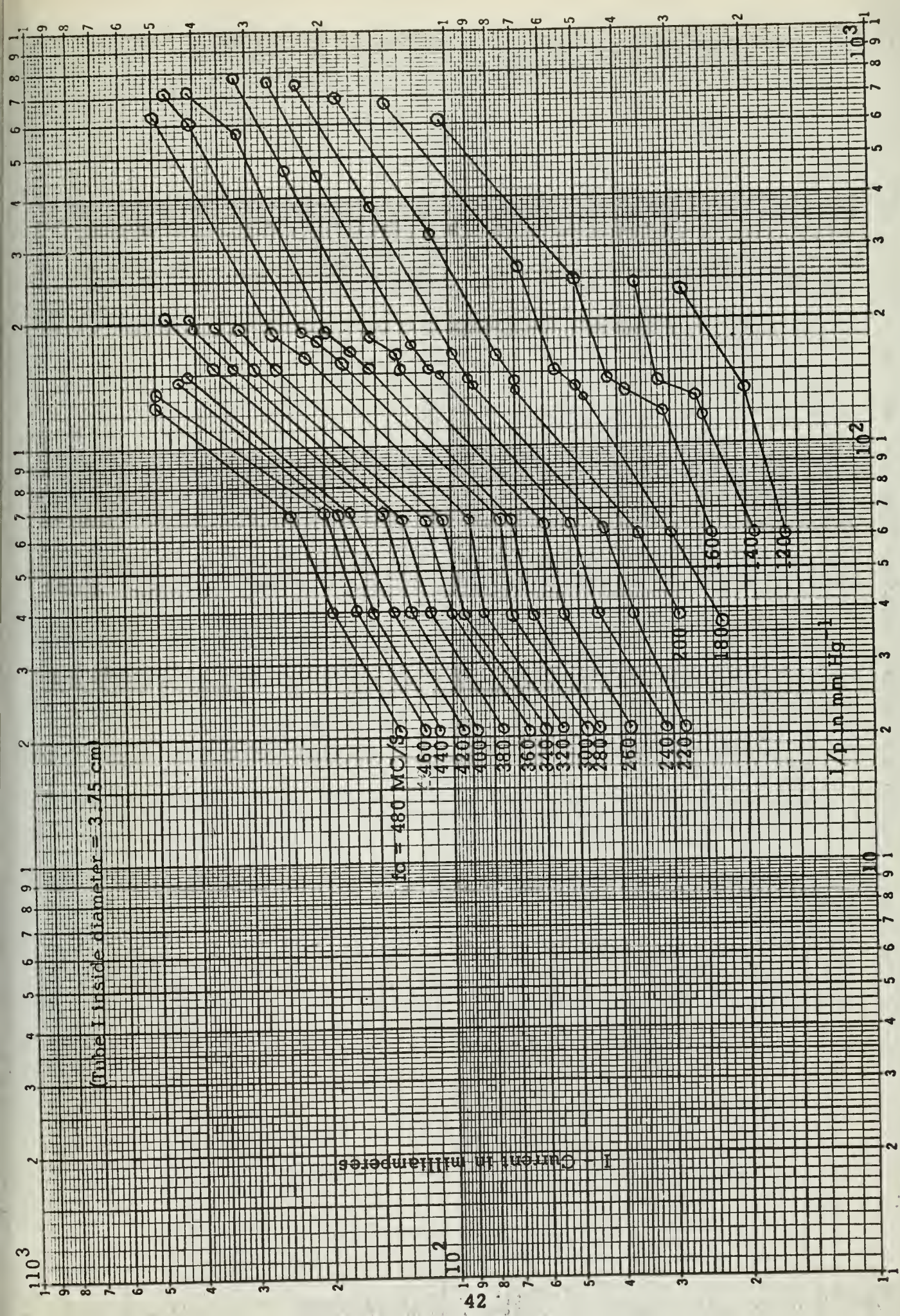


Fig. 14. Current for resonance vs inverse pressure. Argon in Tube I

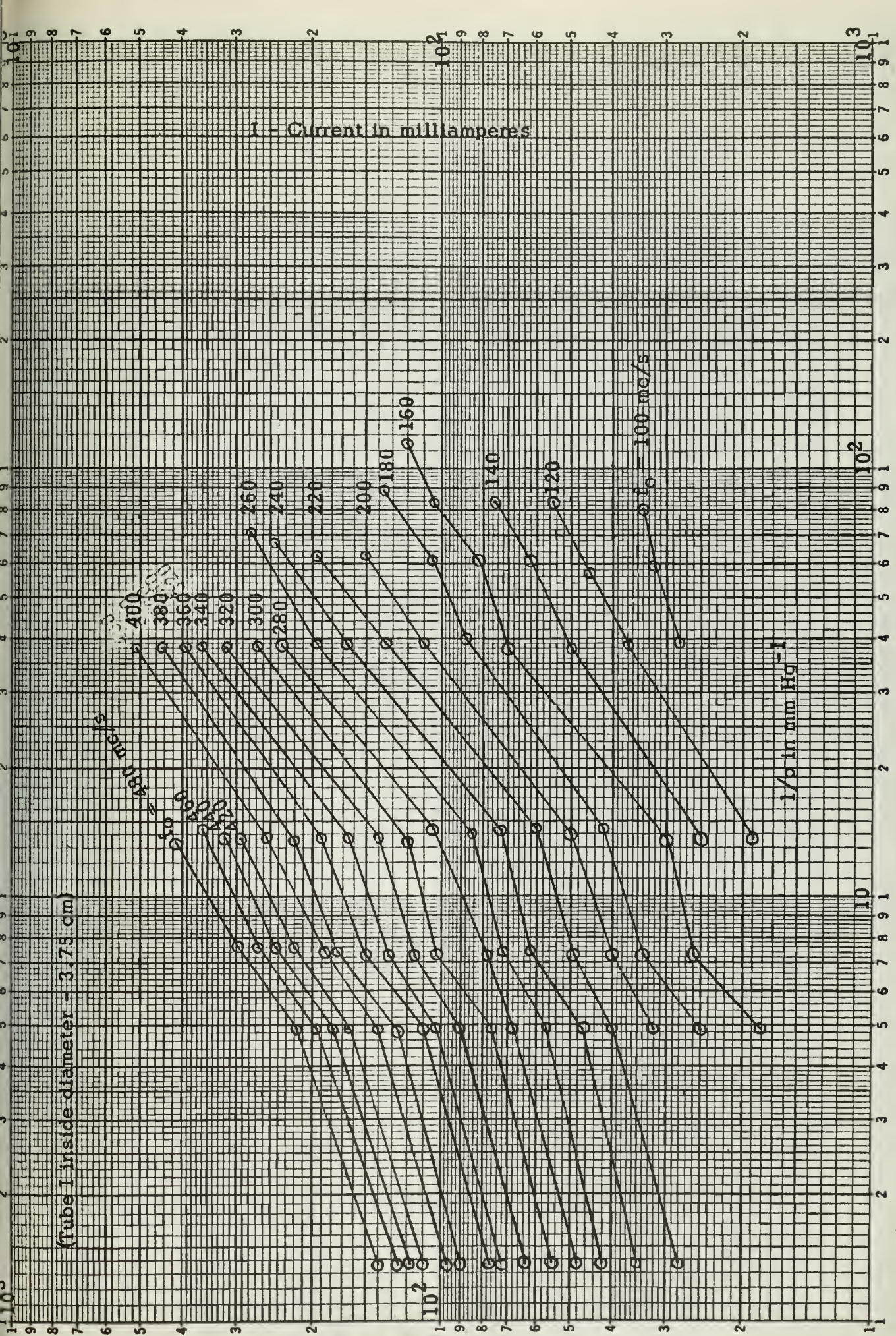


Fig. 15. Current for resonance vs inverse pressure. Neon in Tube I

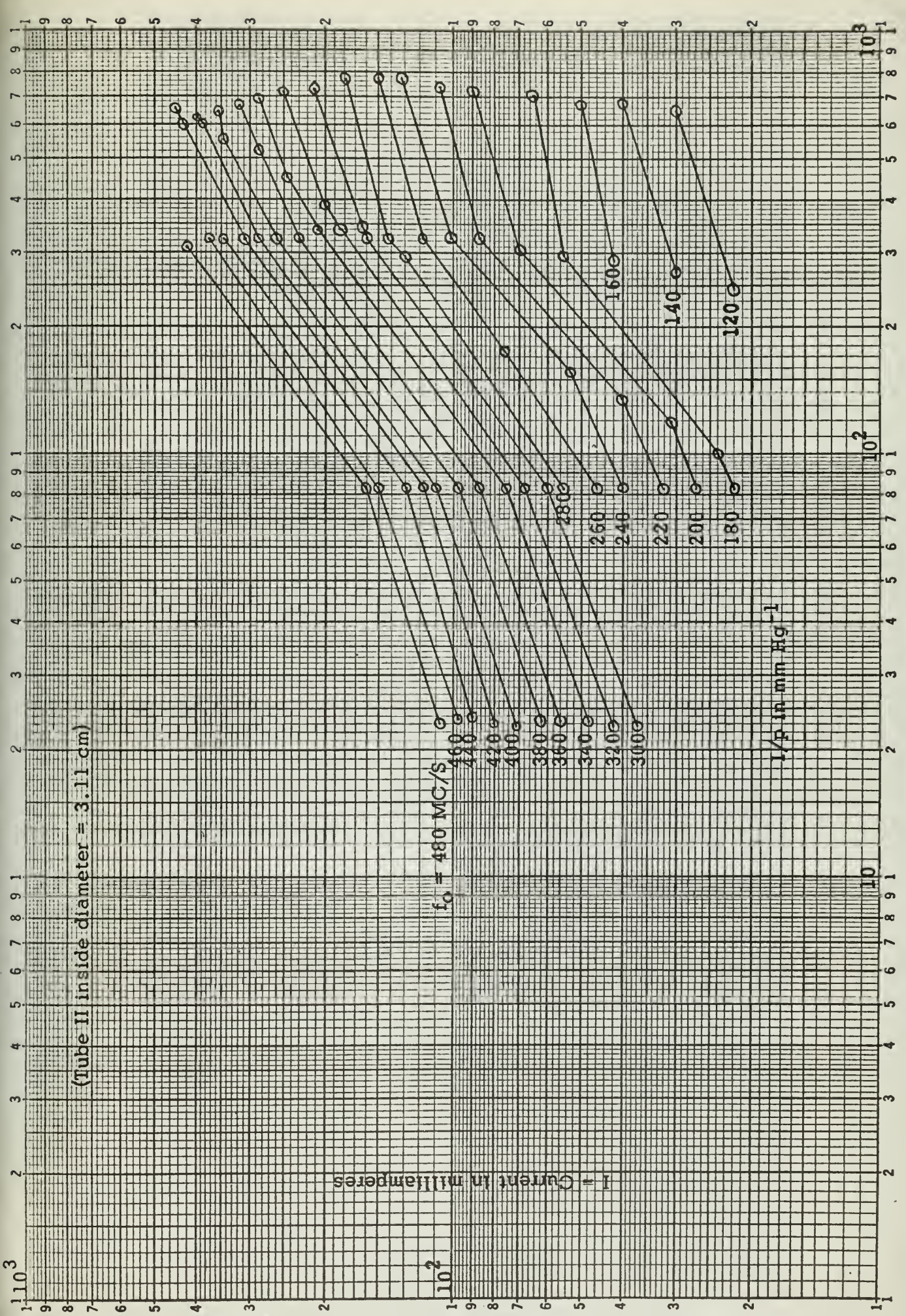


Fig. 16. Current for resonance vs inverse pressure. Argon in Tube II

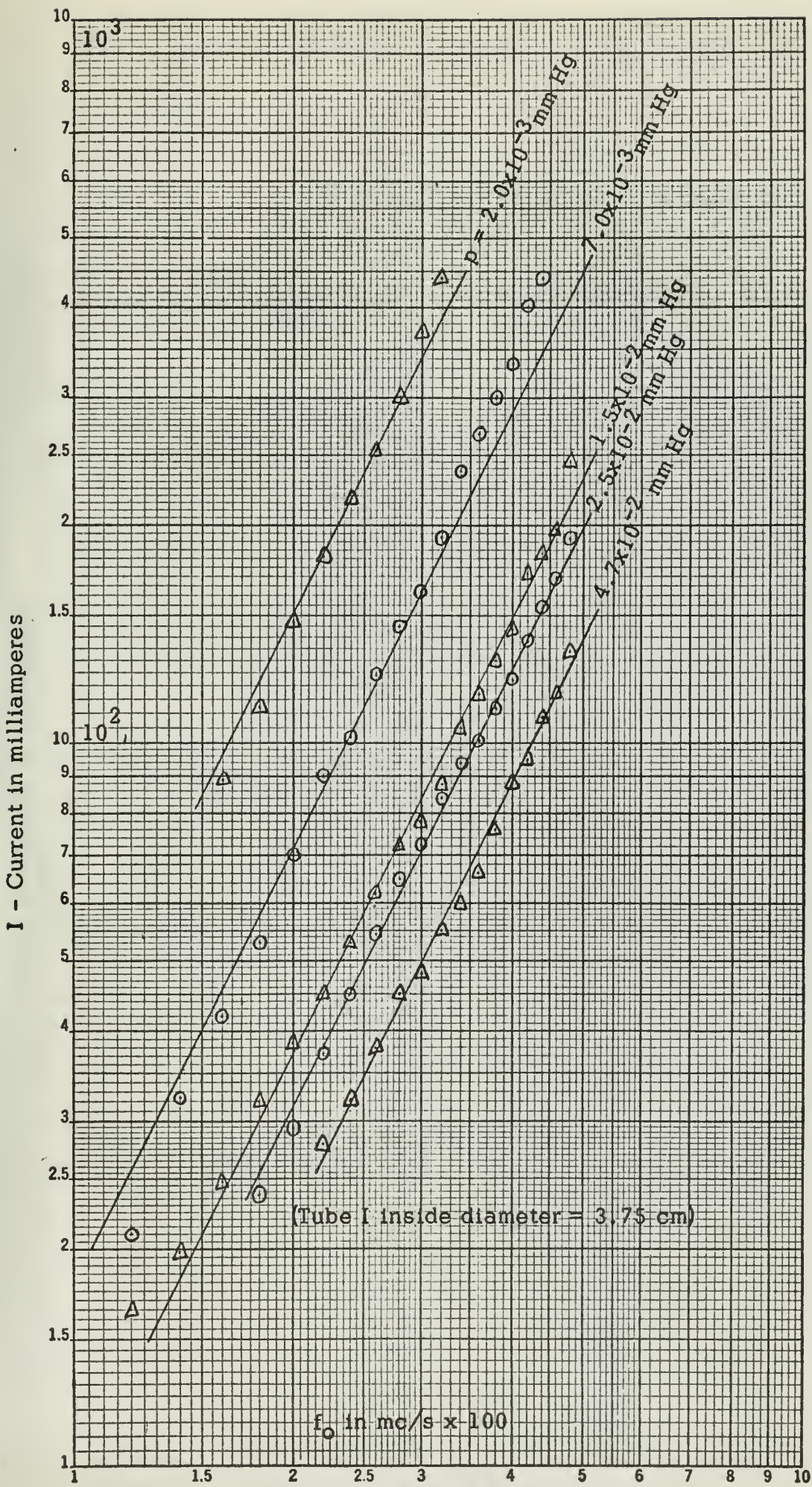


Fig. 17. Current for resonance vs resonant frequency. Argon in Tube I

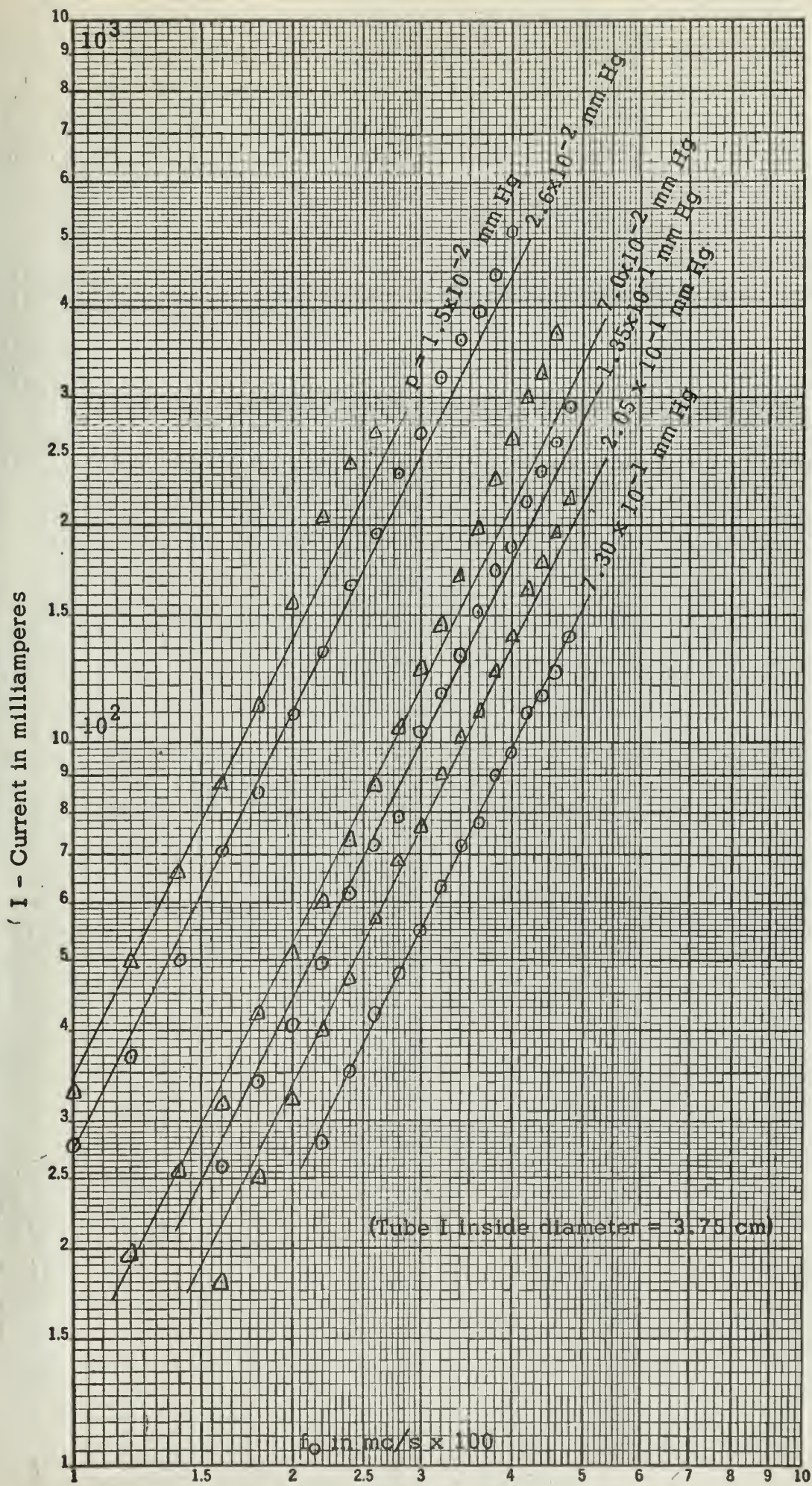


Fig. 18. Current for resonance vs resonant frequency. Neon in Tube I

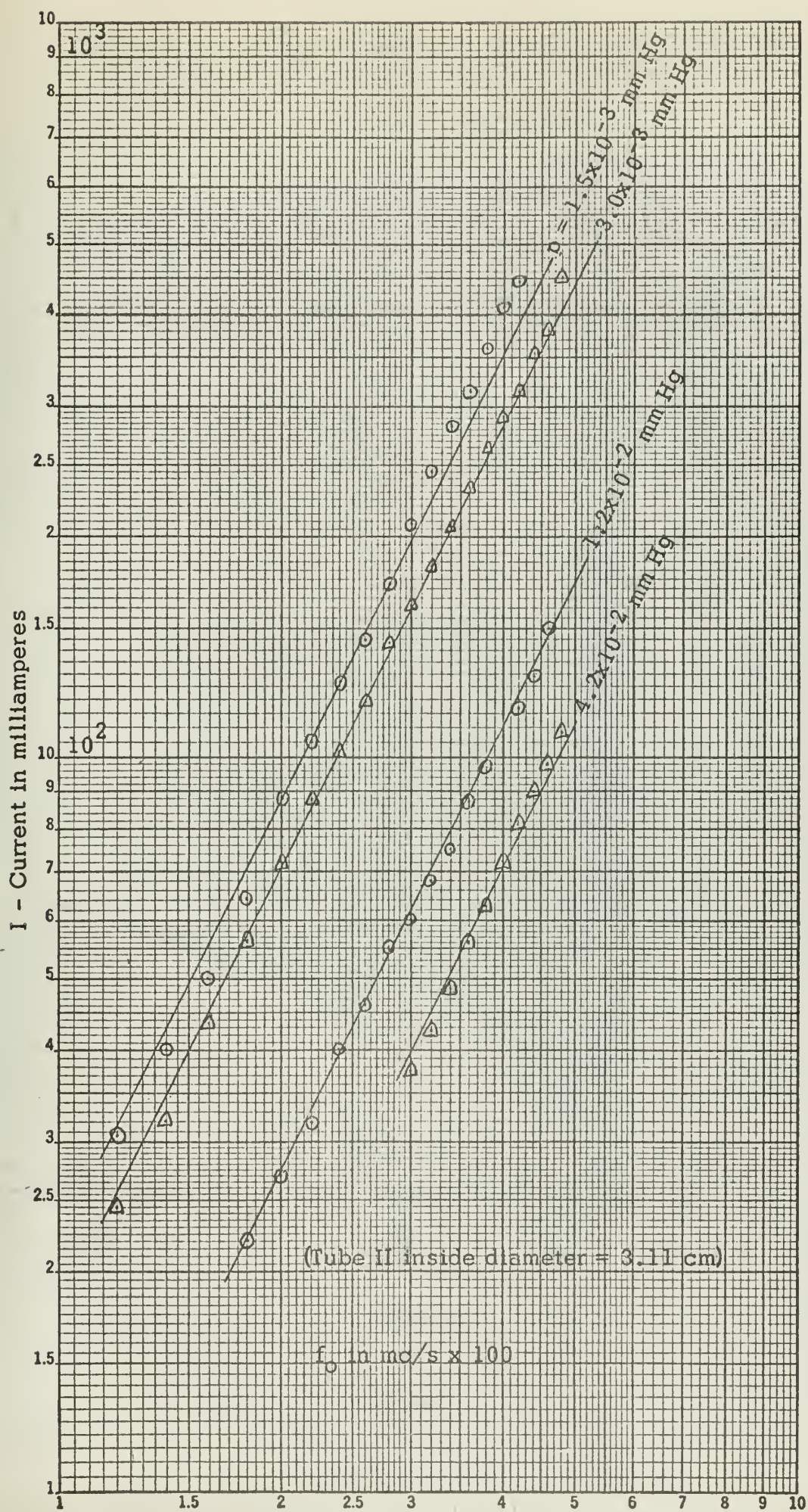


Fig. 19. Current for resonance vs resonant frequency. Argon in Tube II

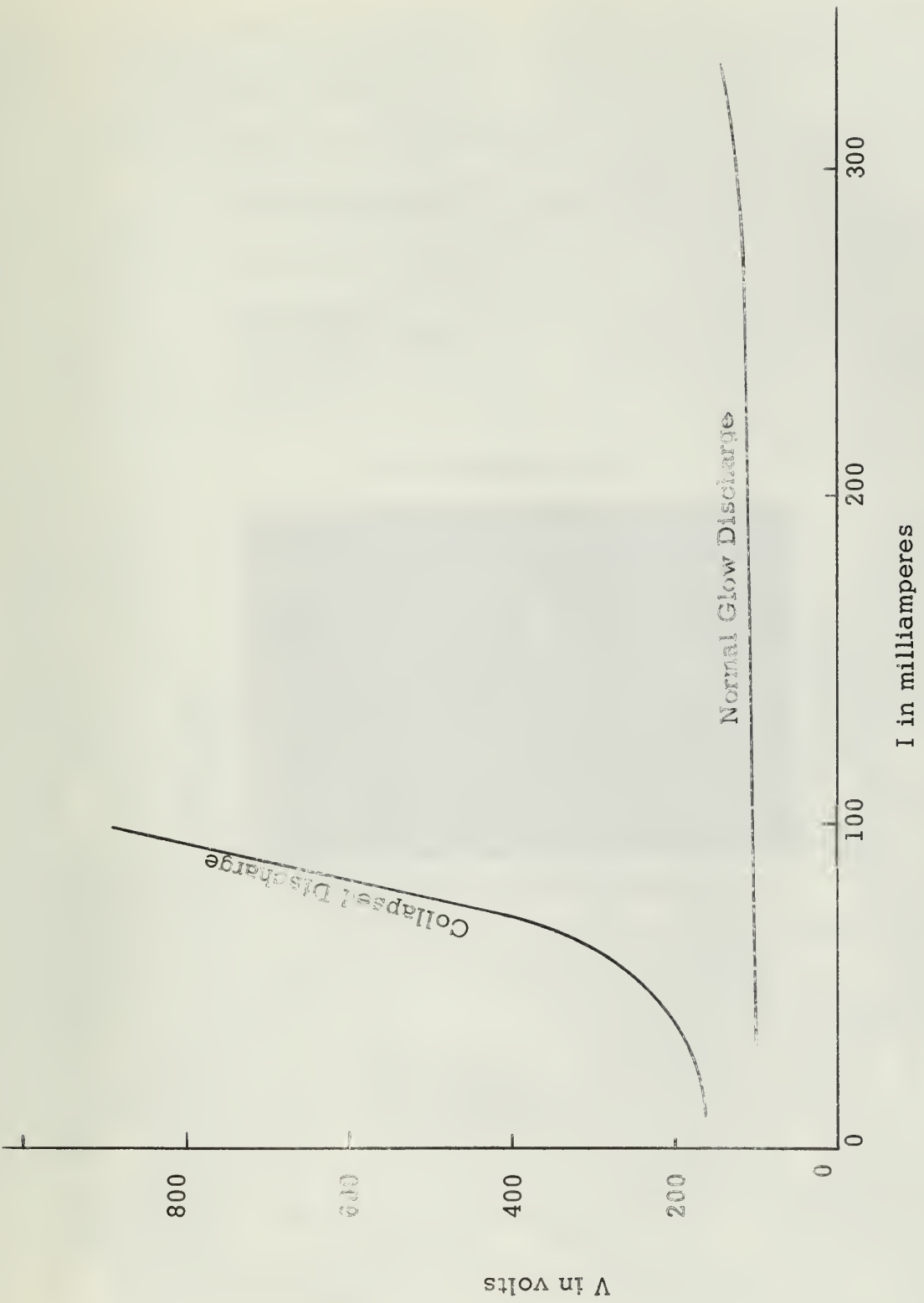


Fig. 20. Tube characteristic for neon at approximately 1×10^{-2} mm Hg.

Tube I

Gas - Argon

Pressure- 1.5×10^{-3} mm Hg

Resonant frequency - f_0 - 220 mc/s

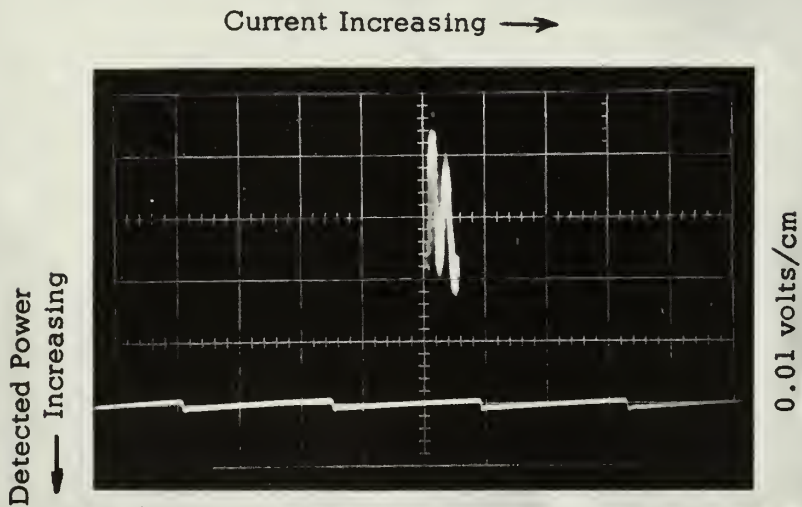
Current - $I = 150$ ma

Lower Trace

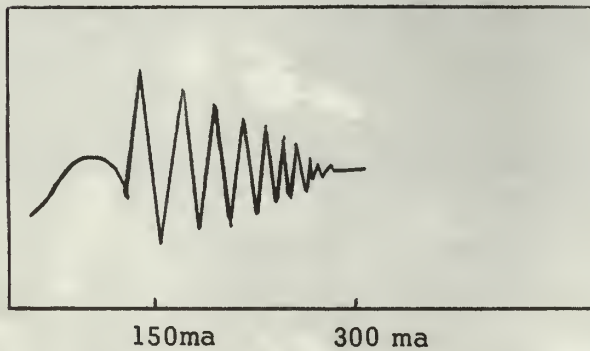
Current waveform

50 ma/cm

400 cps



(a) Oscillogram of portion of resonant response



(b) Sketch of complete resonance

Fig. 21. Anomalous resonance.

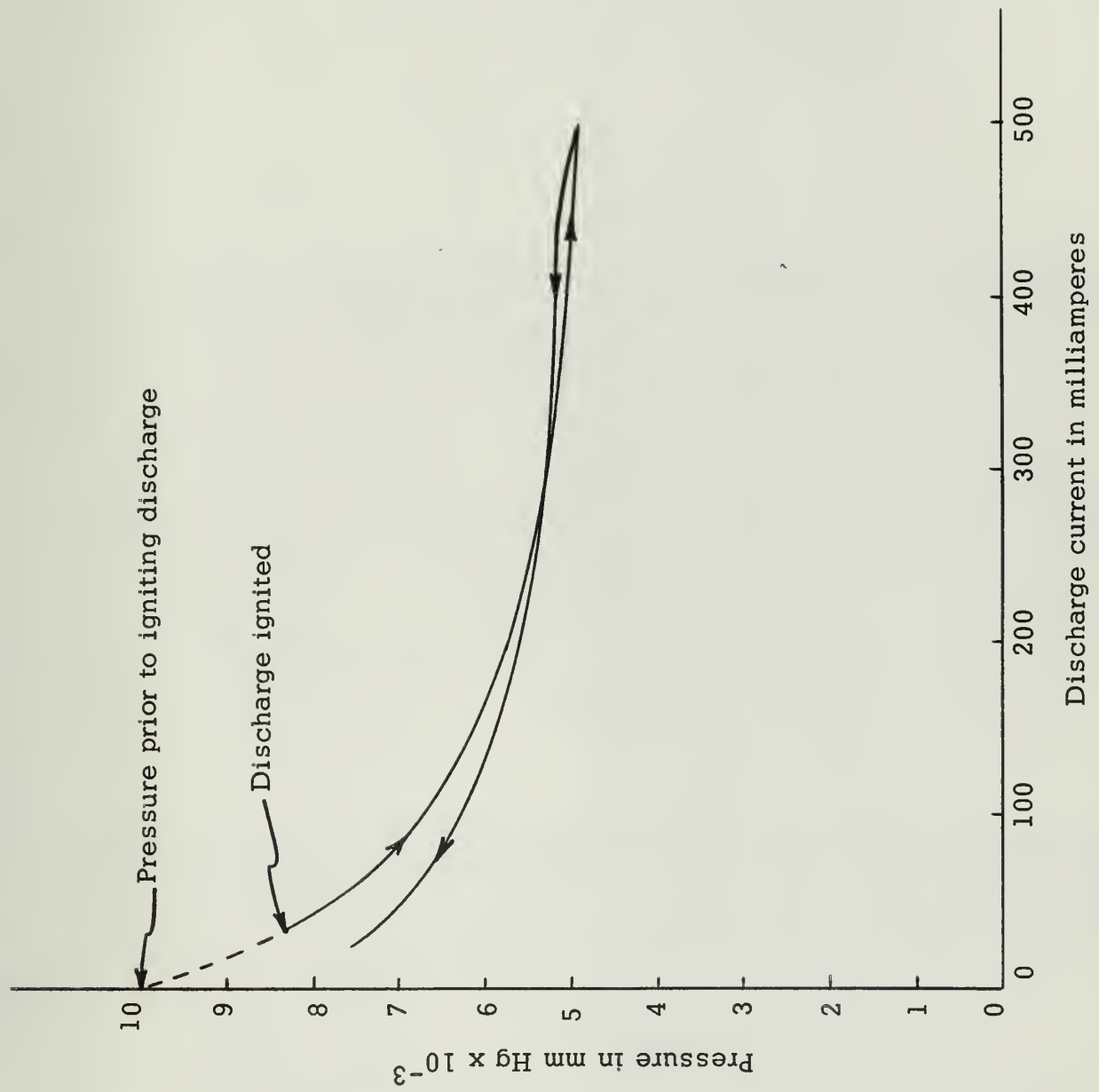


Fig. 22. Variation of pressure with discharge current in argon

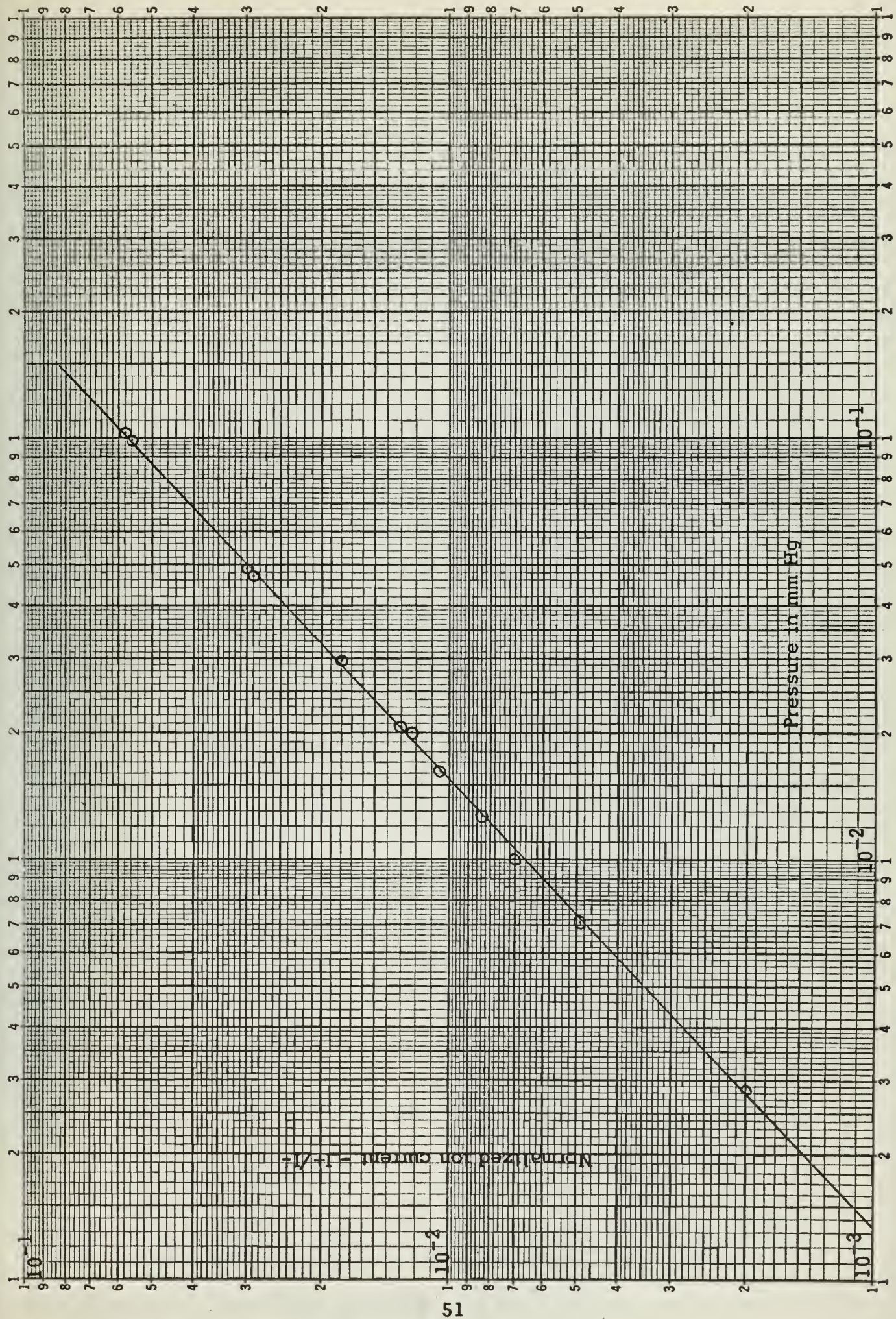


Fig. 23. Calibration curve for argon. Westinghouse 7903 ion gauge

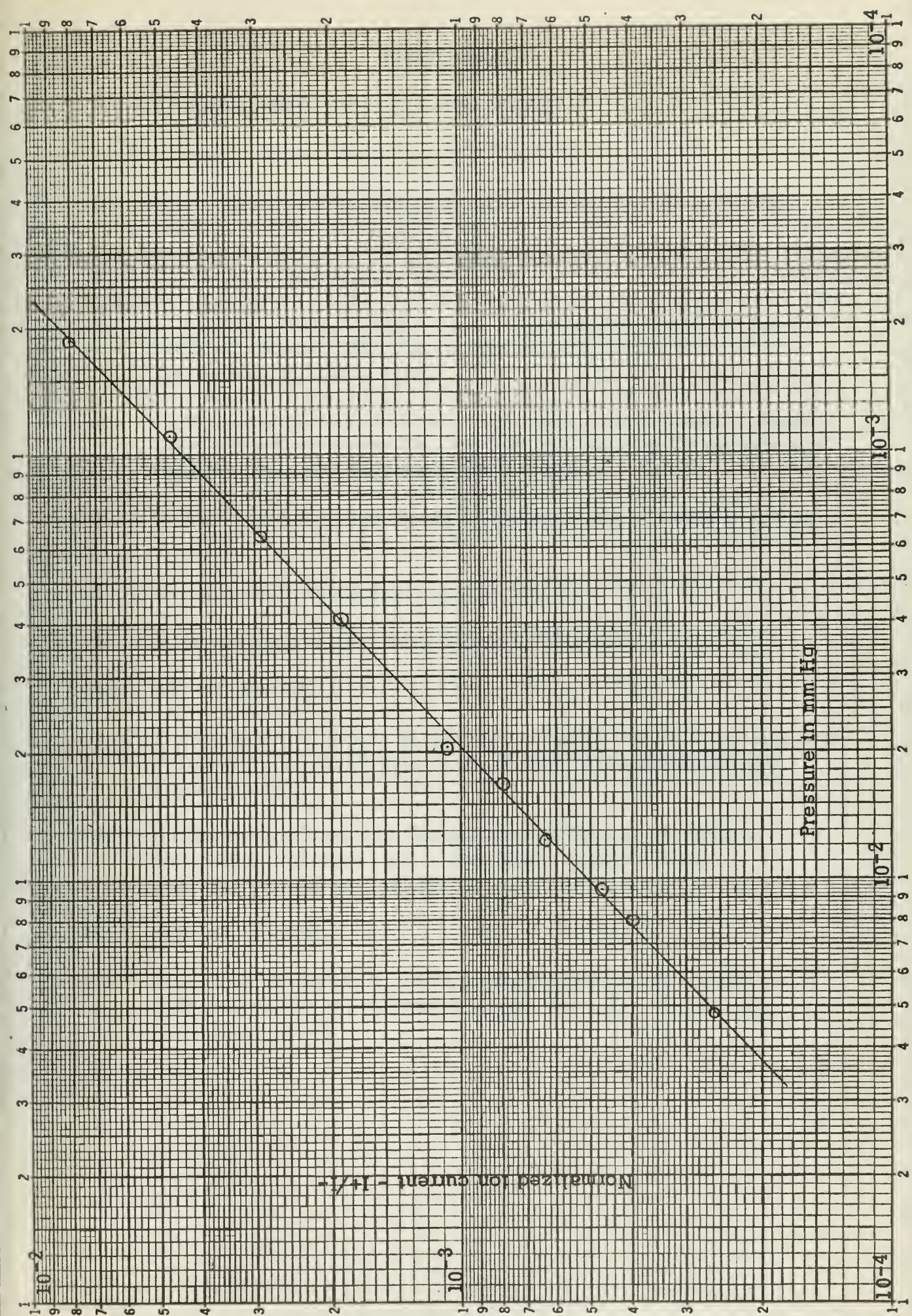


Fig. 24. Calibration curve for neon. Westinghouse 7903 ion gauge

BIBLIOGRAPHY

1. L. Tonks, *Phys. Rev.* 37, 1458 (1931)
2. L. Tonks, *Phys. Rev.* 38, 1219 (1932)
3. W. R. Smythe, *Static and Dynamic Electricity*, McGraw Hill Book Co., New York, (1950) 2nd ed., p. 68.
4. D. Romell, *Nature* 167, 243 (1951)
5. A. Dattner, *Proc. Vth Int. Conf. on Ionization Phen. in Gases*, Munich, (August 1961), North Holland Publishing Co., Amsterdam, 2, 1477, (1962)
6. F. W. Crawford, G. S. Kino, S. A. Self, and J. Spalter, *Micro-wave Laboratory Report No. 961*, W. W. Hanson Laboratories of Physics, Stanford University (Oct. 1962)
7. A. von Engel, *Ionized Gases*, Clarendon Press, Oxford, (1955) p. 104
8. N. Herlofson, *Arkiv Fysik* 3, 247 (1951)
9. R. A. Neilsen, *Phys. Rev.* 50, 950 (1936), Fig. 4.
10. Ref. 9, Fig. 3
11. D. M. Alderson and J. D. Leonard, *Plasma Oscillations in a Low Pressure Neon Discharge*, U. S. Naval Postgraduate School Thesis, (1961)
12. S. Dushman, *Scientific Foundations of Vacuum Technique*, John Wiley and Sons, Inc., New York, (1962) 2nd ed., pp. 649-661 and pp. 665-673.
13. Ref. 10, p. 660
14. G. J. Schulz and A. V. Phelps, *Ionization gauges for measuring pressures up to the millimeter range*, *Rev. Sci. Instr.*, 28, 1051 (Dec. 1957)

APPENDIX

Pressures in the range from 1×10^{-3} to 2×10^{-1} mm Hg were measured with a Westinghouse Type 7903 ion gauge. This is a high pressure triode ionization gauge developed by Shultz and Phelps.¹⁴ The gauge consists of a 5-mil thoriated iridium filament located halfway between two parallel plates ($3/8 \times 1/2$ inch) spaced $1/8$ inch apart. The upper plate is the electron collector and the lower, the ion collector. To insure parallel plane equipotential surfaces between the electrodes the voltage between the electron collector and filament and the voltage between the filament and ion collector are kept equal.

In normal operation a circuit maintains the required voltages on the plates and automatically adjusts the filament current to maintain a specified current to the electron collector. The ion current is then measured and the ratio of ion current to electron current gives the pressure measure when calibrated for the gas used.

It was found that the circuit shown in the Westinghouse instructions did not provide proper regulation of the filament current. However, it was possible to adjust the filament current by hand and operate the gauge.

In this work, the ion collector was maintained at ground potential and the ion current measured with a Keithley micro-microammeter. The filament was maintained at +52 volts and the electron collector at +104 volts. The filament current was adjusted manually at each measurement to maintain 50 microamperes electron collector current. The gauge was

